



1

2

3

4

5

6

7 **Environmental drivers of spatial variability in benthic macrofauna biomass and associated**
8 **carbon fluxes in a large coastal-plain estuary**

9 Authors: Seyi Ajayi^{1*}, Raymond Najjar¹, Emily Rivest², Ryan Woodland³, Marjorie A.M.

10 Friedrichs², Pierre St-Laurent², Spencer Davis¹

11 ¹Pennsylvania State University, University Park, PA, USA

12 ²Virginia Institute of Marine Science, William & Mary, Gloucester Point, VA, USA

13 ³University of Maryland Center for Environmental Sciences, Cambridge, MD, USA

14 *Correspondence to:* Seyi Ajayi (oaa5061@psu.edu)

15

16

17

18

19

20

21

22

23



24 **Abstract**

25 Extensive datasets document the distribution and composition of benthic macrofauna in
26 some estuaries, yet their impact on carbon cycling remains poorly quantified. To address this, we
27 investigated (1) how water chemistry and sediment composition correlate with benthic biomass
28 distribution and (2) the contributions of benthic macrofaunal carbon fluxes to estuarine carbon
29 budgets. We analyzed 8,128 benthic samples collected from Chesapeake Bay (1995–2022) and
30 used generalized additive models to relate observed and modeled environmental variables to the
31 biomass. We also estimated their associated carbon fluxes (calcification and respiration rates)
32 using empirical relationships. The highest biomass was found in the upper Potomac River
33 Estuary and Upper Bay; moderate dissolved oxygen, low salinity, and high nitrate concentrations
34 were the clearest predictors of these zones (explaining 52% of the deviance in biomass). Low
35 surface NO_3^- concentrations within the estuary coincide with high inputs of allochthonous
36 particulate organic carbon (POC) from riverine sources; this POC be the primary food source
37 supporting high biomass zones. In the oligohaline Upper Bay, benthic macrofauna respire 17-
38 50% of total organic carbon available in that region, whereas their contribution is lower
39 downstream. Moreover, the estimated benthic macrofaunal CO_2 production rates from respiration
40 and calcification rates in the Upper Bay ($205 \pm 70 \text{ g C m}^{-2} \text{ yr}^{-1}$) exceeds estimated outgassing
41 ($74.5 \text{ g C m}^{-2} \text{ yr}^{-1}$), suggesting benthic macrofauna contribute significantly to air-sea gas
42 exchange. The explainable spatial distribution of biomass and major role in estuarine carbon
43 cycling highlight the importance and feasibility of incorporating the impacts of benthic
44 macrofauna into numerical models. Refining these models could improve predictions of
45 estuarine responses to natural and anthropogenic changes.

46



47 **1. Introduction**

48 Benthic macrofauna are vitally important to estuarine ecosystems because they can
49 improve water quality, produce and consume organic matter, recycle nutrients, dilute or cycle
50 pollutants, stabilize and transport sediment, and provide food to human populations and other
51 estuarine organisms (Schratzberger & Ingels, 2018; Snelgrove, 1997; Wilson & Fleeger, 2023).
52 As adults, benthic macrofauna often have limited mobility and, in some cases, long life spans,
53 making them reliable indicators of local environmental variability caused by natural and
54 anthropogenic stresses. Their relative abundance and diversity are often used as a proxy to
55 describe the condition of estuaries (Dauer, 1993; Pearson & Rosenberg, 1978; Rosenberg, 1995;
56 Weisberg et al., 1997).

57 ***1.1 Environmental drivers of benthic macrofauna distribution***

58 Because benthic macrofauna are ecologically significant and sensitive to environmental
59 conditions, numerous studies have examined the key factors influencing their distribution in
60 estuaries. Here, we summarize key studies that have investigated how water quality and sediment
61 composition influence benthic macrofauna distribution in estuaries.

62 Dissolved oxygen is one of the primary environmental variables affecting benthic
63 composition; hypoxia (extremely low dissolved oxygen concentration events) significantly
64 degrades the benthic habitat quality (Borja et al., 2008; Diaz et al., 1995; Murphy et al., 2011;
65 Seitz et al., 2009; Woodland & Testa, 2020). Seitz et al., (2009) found that oxygen was the single
66 best predictor of summer benthic biomass by depth in the Chesapeake Bay. In another study of
67 the Chesapeake Bay, dissolved oxygen explains 42% of the variation in the benthic index of
68 biotic integrity (B-IBI), a benthic habitat quality score compiled from multiple factors, including
69 species composition, trophic composition, biomass and abundance, and diversity (Borja et al.,



2008). Similarly in the Baltic Sea, near-bottom oxygen content was among the most important environmental variables shaping benthic communities (Rousi et al., 2019). Among aquatic organisms, benthic macrofauna are the most severely affected by low dissolved oxygen events because they are furthest from the atmosphere, immobile, and coastal sediments are often depleted in oxygen relative to the water column (Dauer & Alden, 1995; Vaquer-Sunyer & Duarte, 2008). Even within benthic communities, vulnerability to hypoxia can vary among taxonomic groups (Vaquer-Sunyer & Duarte, 2008). For example, bivalves are more tolerant of short-term hypoxic stress, which could increase their dominance among benthos as hypoxia increases (Seitz et al., 2009; Vaquer-Sunyer & Duarte, 2008; Woodland & Testa, 2020).

Salinity is also a very important control on benthic community structure (Dauer, 1993; Sturdivant et al., 2013) because different species have different physiological tolerances (Holland et al., 1987; Little et al., 2017; Seitz et al., 2009). In the Humber estuary in the United Kingdom, salinity was amongst the most important environmental variables that contributed to 80% of the biomass variation of the two most dominant bivalve species (Fujii & Raffaelli, 2008). In addition, it was predicted that a 0.3 m rise in sea level would result in a 6.9% loss of benthic macrofaunal biomass, partially due to salinity intrusion.

Ocean acidification, the decrease in seawater pH due to the uptake of atmospheric CO₂, has also negatively affected calcifying organisms in coastal systems. Mollusks (predominately bivalves) are the most strongly affected; ocean acidification decreases their ability to calcify and significantly reduces their survival, growth, development, and abundance (Kroeker et al., 2013). The mechanism of calcification in bivalves will make it difficult for them to adapt to ocean acidification in the future. Bivalves are weak acid-base regulators because they have poorly developed ion exchange mechanisms (Jakubowska & Normant-Saremba, 2015; Thomsen et al.,



93 2015). They are also most susceptible to damage from ocean acidification in their early stages
94 (Jansson et al., 2013). Among other benthic groups, there is a broad variation of sensitivity to
95 variations in pH (Birchenough et al., 2015).

96 Very fine sediment grain size (i.e., high silt-clay fraction & low sand fraction) is
97 associated with lower benthic biomass (Dauer & Alden, 1995; Seitz et al., 2009). A study off
98 Siberia's coast found that sediment grain size is a key predictor of benthic macrofaunal
99 composition, while organic carbon is a key indicator of benthic biomass (Grebmeier et al., 2015).
100 In Chesapeake Bay, Woodland & Testa, (2020) found a negative correlation between
101 accumulated organic matter and benthic biodiversity and a positive association between sediment
102 sand percentage and benthic biodiversity.

103 Food availability has long been known as an important factor influencing benthic
104 biomass (Ehrnsten et al., 2019; Pearson & Rosenberg, 1978). Food availability is driven by
105 primary production in the Bay, which is dominated by phytoplankton in most estuaries (i.e.
106 Chesapeake Bay, Hagy, 2002). A synthesis of shallow, normoxic estuaries worldwide found that
107 as primary production increases, benthic biomass increases (Hagy, 2002; Kemp et al., 2005).
108 However, the timing, size, and location of primary production could lead to hypoxia in the
109 bottom waters, which could have a detrimental effect on the benthos (Dauer et al., 2000; Kemp et
110 al., 2005). In a model of the Baltic Sea, Ehrnsten et al., (2020) predicted that climate change will
111 cause benthic biomass to decrease. However, reduced nutrient loading (due to management
112 efforts) was also predicted to cause the benthic biomass to decrease. Results from the (Ehrnsten
113 et al., 2020) study suggest that the harmful effects of climate change can effectively cancel out
114 the partially positive effects of moderate nutrient loading, perhaps due to increased primary
115 production.



116 In summary, studies theorize that dissolved oxygen, salinity, pH, sediment composition,
117 and primary production are all significant predictors of benthic macrofauna biomass distribution
118 in estuaries.

119 ***1.2 Impact of benthic macrofauna on carbon cycling***

120 Benthic macrofauna biomass influences estuarine biogeochemical cycling, particularly
121 carbon cycling through three major processes: secondary production, respiration, and
122 calcification. Secondary production refers to the consumption of organic matter by benthos to
123 produce soft tissue biomass (Diaz & Schaffner, 1990; Dolbeth et al., 2012; Sturdivant et al.,
124 2013). Secondary production is an important pathway for trophic transfer, as the benthos are
125 eventually consumed by predators or decomposers, with much of the organic carbon ultimately
126 being removed from the estuarine system through advection into the open ocean or burial in
127 sediment (Diaz & Schaffner, 1990; Wilson & Fleeger, 2023). The direct impact of secondary
128 production on carbon cycling is more limited, as involves the transformation of organic matter
129 into biomass rather than shifting carbon between organic and inorganic pools. Respiration is the
130 process by which organic matter and oxygen are consumed, and CO₂, water, and energy are
131 released. As a result, dissolved inorganic carbon (DIC) increases in the water column. During
132 calcification, benthic calcifiers, such as bivalves, uptake bicarbonate and calcium to produce
133 calcium carbonate shells. CO₂ and water are also released as byproducts. However, calcification
134 decreases DIC because bicarbonate utilization exceeds CO₂ production. The removal of
135 bicarbonate also decreases alkalinity (Waldbusser et al., 2013). Together, these processes play a
136 significant role in the carbon budget, with respiration and calcification notably contributing to
137 CO₂ generation (Chauvaud et al., 2003).



138 Studies have quantified the relative contributions of respiration and calcification to
139 estuarine carbon cycling. Respiration has been the most extensively studied. A compilation of
140 data from 20 different estuaries estimated that 24% of total organic inputs to estuaries are
141 respired by benthos, while plankton respiration is generally much lower (Hopkinson & Smith,
142 2004). Macrofauna account for 40% of all benthic respiration (Rodil et al., 2022). Given the high
143 rates of benthic respiration observed in many estuaries, autochthonous primary production alone
144 cannot account for the total organic matter being processed, indicating relatively high
145 allochthonous inputs (Hopkinson & Smith, 2004; Kemp et al., 1997; Schwinghamer et al., 1986).
146 Bivalves, in particular, substantially contribute to benthic respiration and have been thought to
147 significantly decrease the phytoplankton and suspended particulate concentrations in estuaries
148 (Galimany et al., 2020; Nakamura & Kerciku, 2000; Newell & Ott, 2011). Cerco & Noel, (2010)
149 modeled the effect of bivalve filter feeders in the Chesapeake Bay and found that they removed
150 14% to 40% of the carbon load. Beyond respiration, the impact of benthic calcification on
151 estuarine carbon cycling is underexplored (Waldbusser et al., 2013). However recent discoveries
152 of large alkalinity sinks in estuarine tributaries could suggest a large role for bivalves (Najjar et
153 al., 2020). The combined production of CO₂ from respiration and calcification may be a
154 significant contributor to carbon cycling. In San Francisco Bay, this production is estimated to be
155 twice the rate of CO₂ consumption by primary production (Chauvaud et al., 2003). A global
156 extrapolation of the CO₂ generated from calcifying benthos in estuaries is comparable to the
157 magnitude of the total CO₂ emissions from the world's lakes or planetary volcanism (Chauvaud
158 et al., 2003).

159 The absolute fluxes of respiration, calcification, and secondary production can also be
160 estimated from biomass. Multiple studies use empirical relationships to relate benthic biomass to



161 secondary production based on the biomass, taxon, average body mass, water temperature, and
162 other characteristics (Brey, 1990; Chauvaud et al., 2003; Dolbeth et al., 2012; Edgar, 1990;
163 Schwinghamer et al., 1986; Sturdivant et al., 2013; Tumbiolo & Downing, 1994). Secondary
164 production rates are often calculated indirectly because they can be expensive and time-
165 consuming to measure (Sturdivant et al., 2013; Tumbiolo & Downing, 1994). Calcification and
166 respiration rates can be estimated from secondary production using empirical relationships or
167 simple proportional scaling (Chauvaud et al., 2003; Schwinghamer et al., 1986).

168 ***1.3 Focus of this Study***

169 While numerous studies have examined the environmental drivers of benthic biomass in
170 estuaries, most have focused on relatively small spatial and/or temporal scales. Benthic biomass,
171 as opposed to other metrics such as diversity and abundance, is particularly important because it
172 is most directly related to estuarine carbon cycling (Cerco & Noel, 2010; Snelgrove, 1999).
173 Chesapeake Bay is of special interest because the carbon and alkalinity dynamics span the range
174 observed in estuaries and there is extensive historical monitoring data (Najjar et al., 2020). To
175 our knowledge, the most recent studies that specifically linked environmental variables with
176 benthic biomass in the Chesapeake Bay were (Woodland et al., 2021), which focused on these
177 relationships through the lens of forage for higher trophic levels and Seitz et al., (2009), which
178 investigated benthic data from 1996–2004. Woodland & Testa, (2020) also explored the
179 relationship between environmental variables and benthic species diversity in the Bay. However,
180 benthic biomass and biodiversity are not correlated, so our study's results may differ
181 significantly (Alden et al., 2002; Testa et al., 2020). Few studies have also looked at the effect of
182 primary productivity on benthic biomass in the Bay (e.g., Hagy, 2002; Kemp et al., 2005), even



183 though organic matter produced from primary production is considered the main food source for
184 the benthos.

185 The resulting carbon fluxes from benthic macrofauna biomass have large implications for
186 carbon cycling. Although numerous studies have quantified respiration rates in estuaries, very
187 few have provided even rough estimates of calcification (Chauvaud et al., 2003; Waldbusser et
188 al., 2013). Given the potentially important role calcification plays in carbon cycling, addressing
189 this gap is essential for contextualizing the relative contribution of benthic calcification within
190 the broader estuarine carbon budget.

191 In our study, we address the following research questions:

- 192 1) How do water chemistry and sediment composition variables predict the spatial
193 distribution of benthic biomass?
- 194 2) What impact do benthic macrofaunal respiration and calcification have on the carbon
195 budget in estuaries?

196 **2. Methods**

197 ***2.1 Overview***

198 We examined historic benthic macrofauna biomass data collected annually by the
199 Chesapeake Bay Long-Term Benthic Monitoring Program (BMP) (Dauer et al., 2000; Llansó &
200 Zaveta, 2017) and time-averaged the data to emphasize the spatial distribution. To contextualize
201 the benthic biomass data, we used measurements of bottom water temperature, salinity, dissolved
202 oxygen, and sediment sand fraction measured by the BMP at the same time and location as the
203 benthic biomass samples. In addition to these measured environmental variables, we utilized
204 biogeochemical model output from ROMS-ECB, a fully coupled, three-dimensional,
205 hydrodynamic, and estuarine carbon biogeochemistry (ECB) implementation of the Regional



206 Ocean Modeling System (ROMS; Shchepetkin & McWilliams, 2005) developed for the
207 Chesapeake Bay (St-Laurent & Friedrichs, 2024b). We identified correlations between these
208 environmental variables (observed and modeled) and benthic macrofauna biomass using
209 generalized additive models (GAMs). We reviewed the literature to identify empirical
210 relationships between benthic biomass and secondary production, respiration, and calcification
211 fluxes. We used these empirical relationships to quantify the impact of benthic macrofauna on
212 carbon cycling in the Bay.

213 ***2.2 Benthic biomass data***

214 Details of the BMP data we used in our study are described elsewhere (Dauer, 1993;
215 Dauer et al., 2000; Dauer & Lane, 2010; Llansó & Scott, 2011; Llansó & Zaveta, 2017) and are
216 summarized here. The program began in 1984, but consistency in sampling started in 1995,
217 which is when we began our analysis. The sampling occurs mainly in the summer, between July
218 15 and September 30, at both fixed and random stations, with the latter changing location every
219 year. The sampling is conducted by Maryland (Llansó & Zaveta, 2017) and Virginia (Dauer &
220 Lane, 2010) separately, with slightly different protocols used in each state (see below). Our
221 analysis spanned 1995 to 2022, the recent extent of available data, incorporating 28 years of data.

222 The Maryland monitoring program comprises 27 fixed and 150 random stations in the
223 upper Chesapeake Bay. The Virginia monitoring program comprises 21 fixed and 100 random
224 stations in the lower Chesapeake Bay. In Virginia, random stations were not sampled in 1995,
225 and fixed stations were not sampled in 2017 or 2018. Water depths greater than 12 m in the
226 mainstem part of the Bay in Maryland are not sampled because the bottom waters become anoxic
227 in the summer, resulting in azoic sediments. The tributaries are sampled only in the tidal zone;
228 areas with less than 1 m mean lower low water are considered non-tidal. Some locations, such as



229 oyster reefs and other hard substrates, are also not sampled due to gear unsuitability in such
230 habitats. To avoid seasonal biases, we excluded samples collected outside of the summer
231 sampling window of July 15–September 30, as some earlier years included some sampling
232 outside of this window. This selection resulted in a dataset of 8128 samples across both states, or
233 an average of 290 samples per year, slightly less than the maximum of 298.

234 At each sampling station, the uppermost layers of sediment are collected. In Maryland,
235 the sites introduced in 1995 (two fixed sites and all random sites) are sampled with a Young grab,
236 which collects a surface area of 0.0440 m² to a depth of 0.10 m. For the other fixed sites in
237 Maryland, nearshore shallow sandy habitats of the mainstem and tributaries are sampled with a
238 modified box corer with a surface area of 0.0250 m² to a depth of 0.25 m. Muddy habitats and
239 deep-water habitats in the mainstem and tributaries of Maryland are sampled with a Wildco box
240 corer with a surface area of 0.0225 m² to a depth of 0.23 m. The fixed site in the Nanticoke River
241 is sampled with a Petite Ponar grab with a surface area of 0.0250 m² to a depth of 0.07 m. In
242 Virginia, fixed sites use a spade-type box-coring device with a surface area of 0.0182 m² to a
243 depth of 0.02 m; random sites use a Young grab with a surface area of 0.0400 m² to a depth of
244 0.10 m.

245 For both monitoring programs, the sampling contents are sieved through a 0.5 mm screen
246 to retain only benthic macrofauna. The macrofauna are identified at the lowest taxonomical level.
247 The specimens are dried on a pan for at least 24 hours to a constant weight, then a final weight is
248 measured. The specimens are then placed in a muffle furnace for 4 hours at 500°C for ashing,
249 and the specimens are weighed again. The ash-free dry weight (AFDW) is the difference
250 between the dry and ashed weight. We converted the AFDW in g per sample to biomass density
251 B in units of g m⁻² by dividing the AFDW by the area of the sampling device. The data used in



our GAMs analysis include the biomass density of individually selected species and classes and the total biomass density.

To determine the long-term average spatial distribution, biomass densities from all 8128 biomass samples from 1995–2022 were time-averaged onto a grid with cells 0.04° in longitude and 0.03125° in latitude, making the cells nearly square, ~ 3.5 km per side. At least one biomass sample was collected in all 846 cells. Within those cells, the average number of samples per grid cell was 6.62 ± 10.13 (Fig A1). Tributaries and the upper Bay were sampled more densely than the mainstem.

2.3 Bottom water quality data

From the BMP, we used bottom temperature, salinity, and dissolved oxygen data, which are measured with a YSI 660 Sonde or Hydrolab DataSonde 4a in Maryland and a YSI 85 Model meter in Virginia one meter above the sediment surface. Extreme outliers, defined as data points that fall beyond three times the interquartile range from the first or third quartile, were removed. As a result, one value for dissolved oxygen and one for water temperature were excluded from the analysis. The salinity zones are also characterized at each site as tidal fresh (<0.5 ppt), oligohaline (0.5–5 ppt), low mesohaline (5–12 ppt), high mesohaline (12–18 ppt), and polyhaline (>18 ppt); these zones are relatively geographically fixed (with some changes in 2011 due to Hurricane Irene and Tropical Storm Lee) based on long-term averages of salinity (Llansó, 2002; Llansó & Zaveta, 2017). Sediment sand fraction was measured by first collecting two 120 ml benthic grab sub-samples. Sand particles are separated by wet-sieving through a $63\text{-}\mu\text{m}$ stainless steel sieve. Sand fraction is recorded after drying and weighing the samples. The bottom water quality and sediment composition data were time-averaged using the same scheme described earlier for the benthic biomass data.



275 **2.4 Biogeochemical model output**

276 ROMS-ECB output was used to characterize environmental variables not measured by
277 the BMP that could be relevant to predicting the benthic macrofauna biomass distribution.
278 ROMS-ECB uses 20 terrain-following vertical levels and a uniform horizontal resolution of 600
279 m (St-Laurent & Friedrichs, 2024b). We compiled daily averaged output at various grid points
280 from 1995 to 2022 corresponding to the locations of each of the 8128 benthic biomass samples.
281 We selected the ROMS output at the nearest ROMS grid point to each BMP sample location for
282 each variable of interest, described below. Some ROMS-ECB environmental variables are
283 directly linked to primary production. Because the timing of primary production peaks does not
284 always coincide with periods of high food availability for benthos, annual averages may obscure
285 important seasonal patterns. To better capture these temporal mismatches, we calculated both
286 seasonal and annual averages for each variable. For seasonal averages, spring was defined as
287 March–May, summer as June–August, fall as September–October, and winter as December–
288 February. The seasonal and annual averages were then time-averaged in the same scheme
289 explained earlier, resulting in 846 gridded cells.

290 We used ROMS-ECB output, as opposed to Chesapeake Bay Water Quality Monitoring
291 Program (WQMP) data. WQMP has also measured water quality variables since 1984 at over
292 100 tidal stations (Chesapeake Bay Program, n.d.). However, the stations are at different
293 locations than the BMP stations, requiring interpolation to correlate these data with benthic
294 biomass. Other studies have opted to use kriging, a method used to spatially interpolate surface
295 water quality data, to increase the spatial resolution. It has been found to outperform the standard
296 inverse distance weighting tools typically used in the Chesapeake Bay (Murphy et al., 2015).
297 One study evaluated the kriging of surface WQMP data for July 2007 using 117–123 data points



(Murphy et al., 2015). In cross-validation, one measured sample is removed, and the interpolation is then performed at that location; the interpolated value is then compared to the observed value. Cross-validation of temperature, salinity, and dissolved oxygen yielded root-mean-square errors (RMSE) of 0.75 °C, 1.1 ppt, and 1.2 mg L⁻¹, respectively. In contrast, ROMS-ECB output was evaluated with over 500,000 WQMP data points at multiple depths and locations from 1985 to 2021 (St-Laurent & Friedrichs, 2024a). The RMSEs for temperature, salinity, and dissolved oxygen were 1 °C, 1.9 psu, and 1.5 mg L⁻¹, respectively. Although these RMSEs are slightly higher than those from kriging, the evaluation was much more robust, and the long time series evaluation is more relevant to our time-averaging technique over 28 years. In addition, we wanted to utilize bottom water quality data, as these variables are measured closer to the location of benthic macrofauna. However, cross-validation for kriging was only performed at the surface, presumably due to the challenges of accounting for bottom topography in spatial interpolation. For these reasons, ROMS-ECB output was used instead of interpolated WQMP data.

ROMS-ECB simulates many variables, and we considered the subset that might be good predictors of benthic biomass: bottom particulate organic carbon (POC) concentration, bottom total suspended solids (TSS), and surface nitrate (NO₃⁻). POC was considered because a large fraction of POC represents food for benthic macrofauna. TSS was considered a metric of suspended inorganic material, which can inhibit filter-feeding organisms (Grant & Thorpe, 1991). Photosynthesis is largely limited by nitrate in the Chesapeake Bay (Zhang et al., 2021); because phytoplankton productivity and the subsequent sinking of POC is an important source of organic matter to the benthos, nitrate could be a predictor of benthic biomass. ROMS-ECB output was evaluated for robustness with WQMP data using Spearman's rank correlation



coefficient, r_s , which measures the strength of the association between two variables (Hauke & Kossowski, 2011). In our analysis of benthic biomass predictors, we included only variables with r_s above 0.7, which generally indicates a strong association (Akoglu, 2018). NO_3^- was used as it had $r_s = 0.77$, whereas POC and TSS were not as they had $r_s = 0.26$ and 0.24 , respectively (St-Laurent & Friedrichs, 2024a).

We also considered potentially good predictors that could be computed from ROMS-ECB output: surface oxygen supersaturation (ΔO_2) and bottom aragonite saturation state (Ω_{arag}). ΔO_2 can be used as a tracer for net ecosystem production (Herrmann et al., 2020) and hence may indicate organic matter availability to the benthos. Ω_{arag} could predict benthic biomass because bivalve calcification is expected to depend on this metric (Thomsen et al., 2015). $\Delta[\text{O}_2]$ is equal to O_2 minus the saturation concentration, which was computed (as in ROMS-ECB), from temperature and salinity (Garcia & Gordon, 1992). Ω_{arag} is the product of calcium ion concentration and the carbonate ion concentration divided by the solubility product for aragonite, which is a function of temperature, salinity, and pressure. PyCO2SYS (Humphreys et al., 2022) was used to derive the solubility product and carbonate ion concentration from alkalinity, DIC, temperature, salinity, and water depth. We retained ΔO_2 and Ω_{arag} in the analysis because the variables used to compute them can be evaluated with observation (temperature, salinity, DO, alkalinity, and DIC) all had $r_s > 0.7$. Calcium measurements were not available for model evaluation, but calcium is highly correlated to salinity, though deviations may occur at low salinity (Beckwith et al., 2019).

2.5 Statistical modeling

We used GAMs to evaluate how the bottom water quality data and biogeochemical model output predict the spatial distribution of benthic macrofauna biomass. GAMs have been used



344 extensively in ecological research since the late 1960s in coastal ecosystems (Guisan et al., 2002;
345 Smith et al., 2023). GAMs have been shown to perform as well or better than other predictor
346 models based on environmental conditions (Drexler & Ainsworth, 2013). They are data-driven
347 statistical models that find the response to a suite of predictor variables (Grüss et al., 2014;
348 Guisan et al., 2002; Hastie & Tibshirani, 1987; Wood, 2017). They examine how well the
349 predictor (or explanatory) variables explain the ecological response, the strength of the
350 association, and the relative contribution of the different predictors (Guisan et al., 2002). GAMs
351 assume that the multiple functions describing the association between the predictor and response
352 variables are additive and can be smoothed (Guisan et al., 2002). The GAMs package used
353 here— the mgcv library in R with the restricted maximum likelihood (REML) optimization
354 method (Wood, 2011; Wood, 2017)—automates the polynomial order used to fit the smooth
355 function for each predictor variable. An intercept term and an error term are added to the
356 associated smoothed functions for each predictor variable. Model diagnostics include the
357 percentage of deviance explained, signifying how much of the variance in the response variable
358 can be explained by the additive effects of all the smoothed functions associated with the
359 predictor variables. We used GAMs because they are uniquely suited to model the non-linear and
360 non-monotonic relationships between response and predictor variables in our dataset. GAMs
361 require a relatively large amount of data, and with our extensive dataset, they can estimate spatial
362 patterns across a broad geographic region (Grüss et al., 2014; Wood, 2011).

363 To ensure predictor variables in the GAMs analysis were not strongly correlated, we used
364 six variables in the GAMs analysis: total depth, sand fraction, bottom water temperature, bottom
365 salinity, bottom dissolved oxygen, and surface NO_3^- (Table 1). If predictor variables are highly
366 correlated, they distort the GAMs results (Grüss et al., 2014; Grüss et al., 2018; Guisan et al.,



2002). We used Pearson’s correlation coefficients, a common approach for evaluating cross-correlation in GAMs, to evaluate the linear correlation between the predictor variables. If two predictor variables have correlations greater than 0.7, one of the variables was discarded (Dormann et al., 2013). As an alternate means of evaluating multicollinearity, concavity was also analyzed after the smooth functions were applied to the predictor variables. High concavity values (>0.8) indicated that the model might struggle to distinguish between the individual contributions of correlated smooth terms (Wood, 2017). However, applying the Pearson’s correlation coefficient cut-off also eliminated high concavity values (St-Laurent & Friedrichs, 2024a). Ω_{arag} and $\Delta[\text{O}_2]$ were not used as predictor variables because of their high correlation with other predictor variables.

Table 1: Predictor variables from the Chesapeake Bay Benthic Monitoring Program and ROMS-ECB. Information collected from 1995–2022 with annual averages giving every daily average value for the entire period. Seasonal averages were taken for spring (March–April), summer (July–August), fall (September–November), and winter (December–February)

Dataset	Location	Variable	Units	Processing?	Used in GAMs?
BMP	Bottom	DO	mmol m^{-3}	Removed extreme outliers	Yes
BMP	Bottom	Salinity	ppt	None	Yes
BMP	Bottom	Total depth	m	None	Yes
BMP	Bottom	Water temperature	$^{\circ}\text{C}$	Removed extreme outliers	Yes



BMP	Bottom	Sand fraction	%	None	Yes
ROMS-ECB	Surface	NO ₃ ⁻	mmol m ⁻³	Annually and seasonally averaged	Yes
ROMS-ECB	Bottom	POC	mmol m ⁻³	Annually and seasonally averaged	No, model-data validation gave poor results
ROMS-ECB	Bottom	TSS	mg L ⁻¹	Annually and seasonally averaged	No, model-data validation gave poor results
ROMS-ECB	Bottom	Ω _{arag}		Calculated from alkalinity, DIC, temperature, water depth, and salinity using PyCO2SYS. Annually and seasonally averaged	No, highly correlated with salinity
ROMS-ECB	Surface	Δ[O ₂]	mmol m ⁻³	Calculated from oxygen, salinity and temperature using Gracia & Gordon	No, highly correlated with salinity and NO ₃ ⁻



				(1991, 1992). Annually and seasonally averaged	
--	--	--	--	--	--

381 We used Akaike's Information Criterion (AIC), a statistical measure that has been
382 increasingly used in ecology, to evaluate which combination of parameters results in the best
383 model fit (Symonds & Moussalli, 2011). AIC is calculated using the number of fitted parameters
384 in the model, the maximum likelihood estimate, and the residual sum of squares (Symonds &
385 Moussalli, 2011). The model with the lowest AIC value indicates the most parsimonious model
386 with the minimum number of necessary parameters. We chose the predictor variables in our
387 model by minimizing AIC. We generally used annually averaged predictor variables from the
388 ROMS-ECB output because using seasonal averages had a negligible difference on the AIC. To
389 assess the relative influence of each predictor variable, we used Akaike weights, which indicate
390 the probability that a given model is the best among those considered. We ranked models by AIC
391 and summed the Akaike weights for all models containing each predictor variable. Higher
392 Akaike weights indicate stronger support for a variable's inclusion in the best-fitting models.
393 Interaction terms between predictor variables were examined, but their inclusion did not
394 significantly improve the AIC values.

395 We also evaluated the model fit by looking at the distribution of the residuals and a
396 scatter plot of observed vs model response values. A good model would have relatively normally
397 distributed residuals as well and a near 1:1 line in the observed vs model response values.
398 Although GAMs can handle non-normal distributions of the response variable (Guisan et al.,
399 2002), we found the best model fit by applying a natural logarithmic transformation to the
400 biomass. A small constant (0.0001 g m^{-2}) was added to the biomass values before applying the



401 natural logarithmic transformation to account for zeros in the data. The resulting biomass was
402 normally distributed after applying the natural logarithm function, so the GAMs model was fitted
403 with a Gaussian distribution with an identity link function.

404 **2.6 Carbon Flux Estimations**

405 To estimate the relative impact of benthic macrofauna on carbon cycling, we used
406 empirical equations to quantify carbon fluxes, including secondary production, calcification, and
407 respiration.

408 The first step involved converting biomass B (units of g m^{-2}) to a carbon-based biomass
409 B_c (units of g C m^{-2}) using:

$$410 \quad B_c = r_c B \quad (1)$$

411 where r_c is the ratio of carbon mass to total mass in benthic organic matter. In a study on the
412 bivalve filter feeders *Rangia cuneata* and *Corbicula fluminea* that dominate in the tidal fresh and
413 oligohaline waters of the Chesapeake Bay, $r_c = 0.47 \text{ g C g}^{-1}$ was used (Cercio & Noel, 2010). A
414 slightly lower value of 0.41 g C g^{-1} was used in a study of native and introduced bivalves in six
415 North American freshwater systems (Chauvaud et al., 2003). Uncertainties for B_c is derived
416 from the two different r_c values:

$$417 \quad \frac{\Delta B_c}{B_c} = \sqrt{\left(\frac{\Delta r_c}{r_c}\right)^2} \quad (2)$$

418 $\Delta r_c = 0.03 \text{ g C g}^{-1}$, half the range of possible r_c values.

419 We then converted biomass to secondary production rates S (units of $\text{g C m}^{-2} \text{ yr}^{-1}$).

420 Multiple approaches have been used for this conversion, and we used several to be able to
421 broadly quantify uncertainty in our estimates. Some studies assume S is proportional to B_c :

$$422 \quad S_1 = \alpha B_c \quad (3)$$



where the constant of proportionality α is the specific growth rate. We found three studies that estimated α for benthic macrofauna. At the low end, a study of benthic macrofauna in the Chesapeake Bay used $\alpha = 1.06 \text{ yr}^{-1}$ (Wilson & Fleeger, 2023). At the high end, a study of *C. fluminea* used $\alpha = 4.45 \text{ yr}^{-1}$ (Chauvaud et al., 2003). An intermediate value of $\alpha = 2 \text{ yr}^{-1}$ was based on monthly observations of benthic macrofauna dominated by the crustacean *Corophium volutator* and the bivalve *Limecola balthica* at an intertidal site in the upper Bay of Fundy (Schwinghamer et al., 1986). A mean value of 2.50 yr^{-1} was used in Eq. 3. The uncertainty for S_1 is derived from B_c and α :

$$\frac{\Delta S_1}{S} = \sqrt{\left(\frac{\Delta \alpha}{\alpha}\right)^2 + \left(\frac{\Delta B_c}{B_c}\right)^2} \quad (4)$$

$\Delta \alpha$ is half the range of possible α values and equals 1.695 yr^{-1} . Temperature dependence for bivalve secondary production was included by Edgar (1990):

$$S_2 = S_0 \left(\frac{B}{1 \text{ g m}^{-2}}\right)^{0.87} \left(\frac{T}{1 \text{ }^\circ\text{C}}\right)^{0.46} \quad (5)$$

where $S_0 = 0.40 \text{ g m}^{-2} \text{ yr}^{-1}$. Note that the coefficient at the beginning of the equation differs from that of Edgar (1990) because of a change in units of B from mg to g m^{-2} and of S from mg C d^{-1} to $\text{g C m}^{-2} \text{ yr}^{-1}$. This equation has been shown to agree well with direct secondary production and biomass measurements (Sturdivant et al., 2013). Tumbiolo & Downing (1994) developed Eq. 6, and the model was also validated with direct calculations of production in the Chesapeake Bay:

$$\log_{10}(S_3) = \beta_0 + b \log_{10}\left(\frac{B}{1 \text{ g m}^{-2}}\right) - m \left(\frac{M}{1 \text{ mg}}\right) + t \left(\frac{T}{1 \text{ }^\circ\text{C}}\right) - z \log_{10}\left(\frac{Z}{1 \text{ m}} + 1\right) \quad (6)$$

where $\beta_0 = 0.24, b = 0.96, m = 0.21, t = 0.03, z = 0.16$. In this calculation, we used the AFDW of biomass for B . The bottom water temperature (T) was measured only in the summer on the same day the benthic samples were collected. This reliance on summer bottom water



temperatures may be slightly inaccurate, as it reflects summer production scaled up to annual values. For max individual body mass (M), we used the maximum weight of the bivalve *R. cuneata* collected in a study in the Choptank River in the Chesapeake Bay, which was 5953 mg (Hartwell et al., 1991). Z corresponds to the water depth. The Edgar (1990) and Tumbiolo & Downing (1994) secondary production equations do not include explicit sources of uncertainty. The mean S value was calculated from the three different secondary production equations (Eqs. 3, 5, and 6) and uncertainty arises from the multiple equations used:

$$\frac{\Delta S}{S} = \sqrt{w_3 \left(\frac{\Delta S_1}{S_1} \right)^2 + w_5 \varepsilon + w_6 \varepsilon} \quad (7)$$

where w corresponds to the weights associated with the uncertainty for each secondary production calculation. The subscripts in w correspond to the secondary production equations (Eqs. 3, 5, and 6), with values of 0.1 for w_3 , 0.45 for w_5 , and 0.45 for w_6 . Higher weights were assigned to w_5 and w_6 since the associated secondary production equations have been more extensively validated. Since there is no well-defined source of uncertainty in these two equations, a small error term ε of 0.001 was included.

We then calculated calcification rates from secondary production rates. We relied on a study by Chauvaud et al. 2003, which calculates the ratio of shell production ($\text{g CaCO}_3 \text{ m}^{-2} \text{ yr}^{-1}$) to tissue production ($\text{g C m}^{-2} \text{ yr}^{-1}$):

$$C = \gamma_{\text{CO}_2} r_s S \quad (8)$$

where r_s is the ratio of shell production to tissue production. The study samples the bivalve *Potamocorbula amurensis* in the northern San Francisco Bay. The ratio of shell production to tissue production was 10. There was also a ratio of 15 cited for the bivalve *C. fluminea*, a more relevant species to our study, but the reference is from unpublished data. Calcification C (units of



g C m⁻² yr⁻¹) is in terms of CO₂ produced as calcification shifts seawater equilibrium and produces dissolved CO₂. γ_{CO_2} corresponds to the ratio of the mass of CO₂ produced divided by the mass of calcium carbonate produced. Chauvaud et al., (2003) gives a ratio of 0.12 for the bivalve *C. fluminea* and 0.09 for the bivalve *P. amurensis*. For the two bivalve species, the product of the ratio of shell production to tissue production (r_s) and the ratio of mass of CO₂ produced divided by calcium carbonate produced (γ_{CO_2}) gives an average value of 1.35; this value was used in Eq. 8. Calcification uncertainty is derived from γ_{CO_2} , r_s , and S :

$$\frac{\Delta C}{C} = \sqrt{\left(\frac{\Delta k}{k}\right)^2 + \left(\frac{\Delta S}{S}\right)^2} \quad (9)$$

where k is the product of r_s and γ_{CO_2} , with one value for *C. fluminea* and one for *P. amurensis*. $\Delta k = 0.45$ and is half the range of possible k values.

We also calculated respiration rates from secondary production. A ratio of respiration rates to secondary production rates was derived from an empirical relationship between benthic macrofauna biomass and respiration rates in the Bay of Fundy study referenced earlier:

$$\log_{10} \left(\frac{R}{1 \text{ kcal m}^{-2} \text{ yr}^{-1}} \right) = \alpha_0 + s \log_{10} \left(\frac{S}{1 \text{ kcal m}^{-2} \text{ yr}^{-1}} \right) \quad (10)$$

where $s = 0.993$ and $\alpha_0 = 0.367$. Kcal were converted to grams of carbon, using the ratio 1 g C=11.4 kcal (Chauvaud et al., 2003). The estimations for calcification and respiration rates have less data validation than secondary production. However, we are confident they can approximate the relative carbon flux impact of the benthic macrofauna. The uncertainty in respiration rates is derived solely from S :

$$\frac{\Delta R}{R} = \ln(10) S \frac{\Delta S}{S} \quad (11)$$



Eq. 12 shows that the total CO₂ generated, TC, is the sum of the CO₂ generated from respiration and calcification (units of g C m⁻² yr⁻¹) (Chauvaud et al., 2003).

$$TC = C + R \quad (12)$$

The uncertainties in TC are derived from C and R:

$$\Delta TC = \sqrt{(\Delta C)^2 + (\Delta R)^2} \quad (13)$$

We grouped the biomass measurements and associated carbon fluxes into 12 regions to highlight broader spatial differences. These regions were created by combining the 92 segments delineated by the Chesapeake Bay Program (CBP; 2004). The 12 regions were the Patuxent River, the Potomac River, the Rappahannock River, the York River, the James River, the Western Shore (the small western tributaries in Maryland), the Eastern Shore (all tributaries east of the mainstem), the Upper Bay (mainstem oligohaline zone and tidal fresh zones or CB1 and CB2), the Mid Bay (mainstem mesohaline zones or CB3, CB4, and CB5), and the Lower Bay (mainstem polyhaline zones or CB6, CB7, and CB8). Biomass density values were calculated for each region.

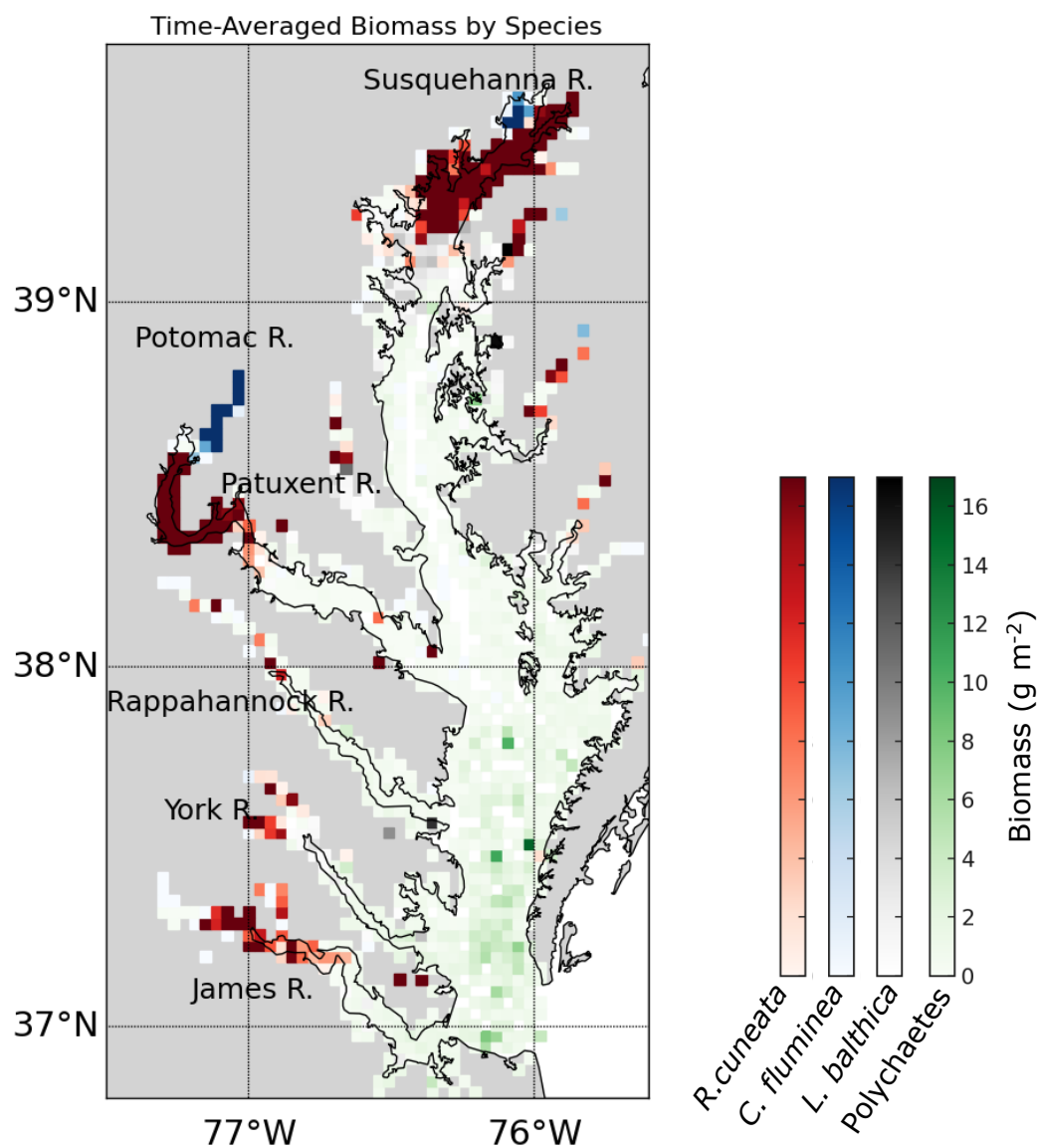
3. Results

3.1 Spatial distribution of benthic macrofauna biomass

Benthic macrofauna biomass exhibits strong spatial variability across the Chesapeake Bay, with higher concentrations in the tidal fresh and oligohaline zones, and lower concentrations in the Mid Bay and lower sections of many tributaries. Figure 1 shows the spatial distribution of the time-averaged (1995–2022) summer benthic macrofauna biomass. The arithmetic mean of all biomass measurements (based on the full data set, $N = 8128$) is 7.93 g m⁻², whereas the spatial mean is 6.31 g m⁻² ($N = 846$). The sampling scheme oversamples tributaries (Fig. A1) where more biomass is concentrated, inflating the arithmetic mean. The standard



509 deviation of the full dataset is 28.70 g m^{-2} , indicating that the distribution is heavily skewed to
510 the right, with the highest sample reaching up to 722 g m^{-2} . The standard deviation of the time-
511 averaged data is 17.02 g m^{-2} , considerably smaller than the full data set since it does not include
512 temporal variability, but is nevertheless still skewed to the right, with the highest gridded value
513 of 220.18 g m^{-2} . Most of the high biomass density zones ($>30 \text{ g m}^{-2}$) are concentrated in the tidal
514 fresh and oligohaline sections of the mainstem and Potomac River. The other tributaries have
515 higher biomass in the tidal fresh and oligohaline and zones compared to the other salinity zones.
516 In the Mid Bay and lower sections of many tributaries, biomass is very low.



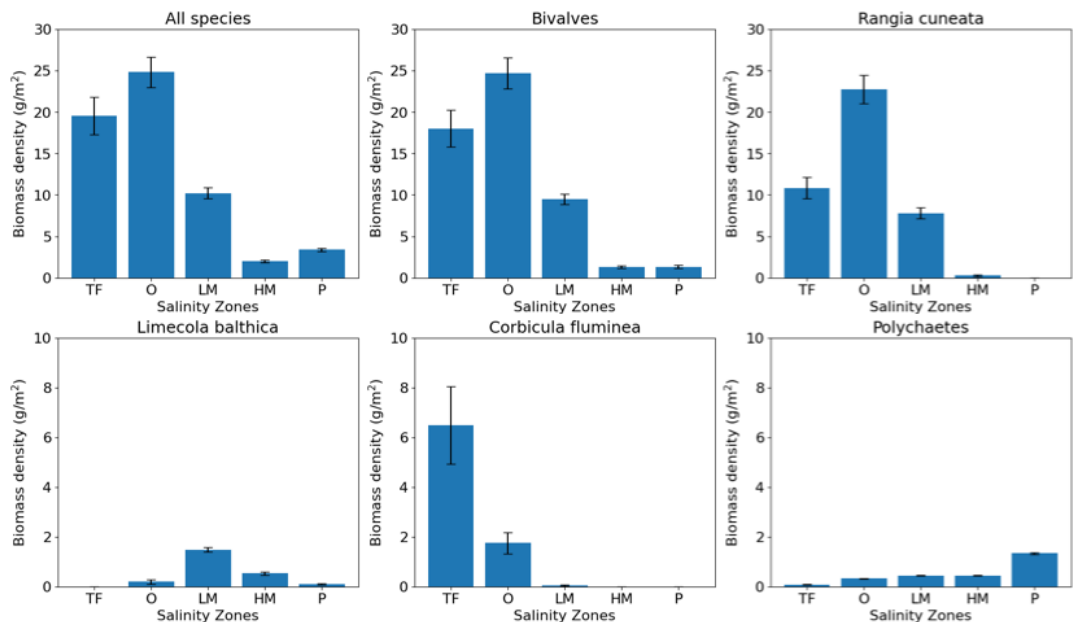
517

518 Figure 1: Average summer biomass density from 1995 to 2022 from the Maryland and Virginia
 519 Benthic Monitoring Program. Each color corresponds to a specific bivalve species (*M. balthica*,
 520 *C. fluminea*, or *R. cuneata*) or polychaetes. The color shown on the map is the species with the
 521 highest time-averaged biomass in that grid cell.

522



523 In the high-biomass tidal fresh and oligohaline zones, bivalves dominate; whereas
524 polychaetes are more prevalent in the lower-biomass mesohaline and polyhaline zones. The
525 distribution of benthic biomass density into salinity zones for multiple taxonomic groups and
526 species is shown in Fig. 2. Bivalves comprise 88.0% of the benthic biomass, and polychaetes
527 comprise 7.3%. At a taxonomic species level, the bivalve *R. cuneata* comprises 66.1% of the
528 biomass, followed by the bivalve *C. fluminea* (8.0%) and the bivalve *L. balthica* (7.5%). The
529 high biomass zones in the Upper Bay, Potomac River, and James River are dominated by *R.*
530 *cuneata*, mostly in the oligohaline zone (Fig. 2). *C. fluminea* also dominates in relatively higher
531 quantities in the tidal fresh zone of the Potomac River and the tidal fresh zone of the Upper Bay
532 (Fig. 2). In general, *R. cuneata* has a higher biomass density in the tidal fresh than *C. fluminea*
533 because *R. cuneata* is present in all tidal fresh zones. *L. balthica* is distributed in multiple salinity
534 zones; it is highest in the lower mesohaline and is the dominant species in the lower mesohaline
535 zone of the Upper Bay and Patuxent River. The biomass density of *L. balthica* in the lower
536 mesohaline ($<2 \text{ g m}^{-2}$) is significantly lower than *C. fluminea* and *R. cuneata* in the tidal fresh
537 and oligohaline zones. Polychaetes are the species that dominate over the largest geographic
538 area, throughout the polyhaline and part of the higher mesohaline (Fig. 1 & 2). However, their
539 biomass density is low relative to bivalves ($<2 \text{ g/m}^2$). Bivalves are sparse throughout the higher
540 mesohaline and polyhaline zones.



541

542 Figure 2: Average summer benthic biomass density of multiple classes and species in each
543 salinity zone from 1995 to 2022. The salinity zones are determined by the BMP program based
544 on the long-term average of salinity in each geographic zone: TF (Tidal Freshwater) 0–0.5 ppt,
545 OH (Oligohaline) 0.5–5 ppt, LM (Low Mesohaline) 5–12 ppt, HM (High Mesohaline) 12–18
546 ppt, and Polyhaline (PO) ≥ 18 ppt. Averages and standard errors (bars) are computed using the
547 full data set, not the gridded values. Note difference in vertical scale between upper row and
548 lower row.

549 **3.2 Correlation of environmental variables with biomass**

550 The GAMs analysis revealed key drivers of benthic biomass both at the community level
551 (all taxa combined) and for specific taxonomic groups and species. The results for total benthic
552 biomass (all taxa), polychaetes, and the bivalve species *R. cuneata*, *C. fluminea*, and *L. balthica*
553 are shown in Table 2. The bivalve group was excluded from the table because its results were
554 nearly identical to total benthic biomass results. For total benthic biomass, the predictor variables



555 explain 54.9% of the deviance in biomass. For individual taxa, the predictive capability of
 556 GAMs increases, with 73.7% of *R. cuneata* biomass deviance explained by the predictor
 557 variables. For total benthic biomass, dissolved oxygen was the most influential predictor variable
 558 (highest summed Akaike weight), followed by total depth, salinity and NO_3^- . Although, water
 559 temperature and sand fraction were included in the model, they had relatively little influence. For
 560 individual taxa, dissolved oxygen became less influential, especially for *R. cuneata* and *C.*
 561 *fluminea*. Salinity generally increased in influence as a predictor variable for species-specific
 562 models most notably for *C. fluminea*. NO_3^- also generally increased in influence as a predictor
 563 variable for species-specific models, with very high influence as a predictor of *C. fluminea*
 564 biomass.

565 Table 2: This table presents the best-fitting generalized additive model (GAM) for each taxa
 566 assemblage, determined by minimizing Akaike's Information Criterion (AIC). Summed Akaike
 567 weights indicate the relative importance of each predictor variable across all models considered,
 568 with higher values suggesting stronger support for a variable's inclusion in the best-fitting
 569 models. "N/A" indicates that the variable was not included in the best model. Some variables
 570 may have high summed Akaike weights even if they are not in the best-fitting model. For
 571 example, in the *R. cuneata* model, DO has a summed Akaike weight of 0.571, while water
 572 temperature has 0.032. In the *C. fluminea* model, DO has 0.384, and total depth has 0.24.

Taxa	N	Deviance Explained	Summed Akaike Weight					
			DO	Salinity	Total Depth	Water temperature	Sand fraction	NO_3^-



All taxa	846	54.9%	0.536	0.032	0.400	0.000	0.000	0.031
Polychaetes	846	50.0%	0.457	0.173	0.266	N/A	0.000	0.104
<i>R. cuneata</i>	846	73.7%	N/A	0.161	0.183	N/A	0.024	0.059
<i>C. fluminea</i>	846	65.9%	N/A	0.212	N/A	0.122	0.078	0.132
<i>L. balthica</i>	846	58.4%	0.888	0.000	0.112	N/A	0.000	0.000

573

574

575

576

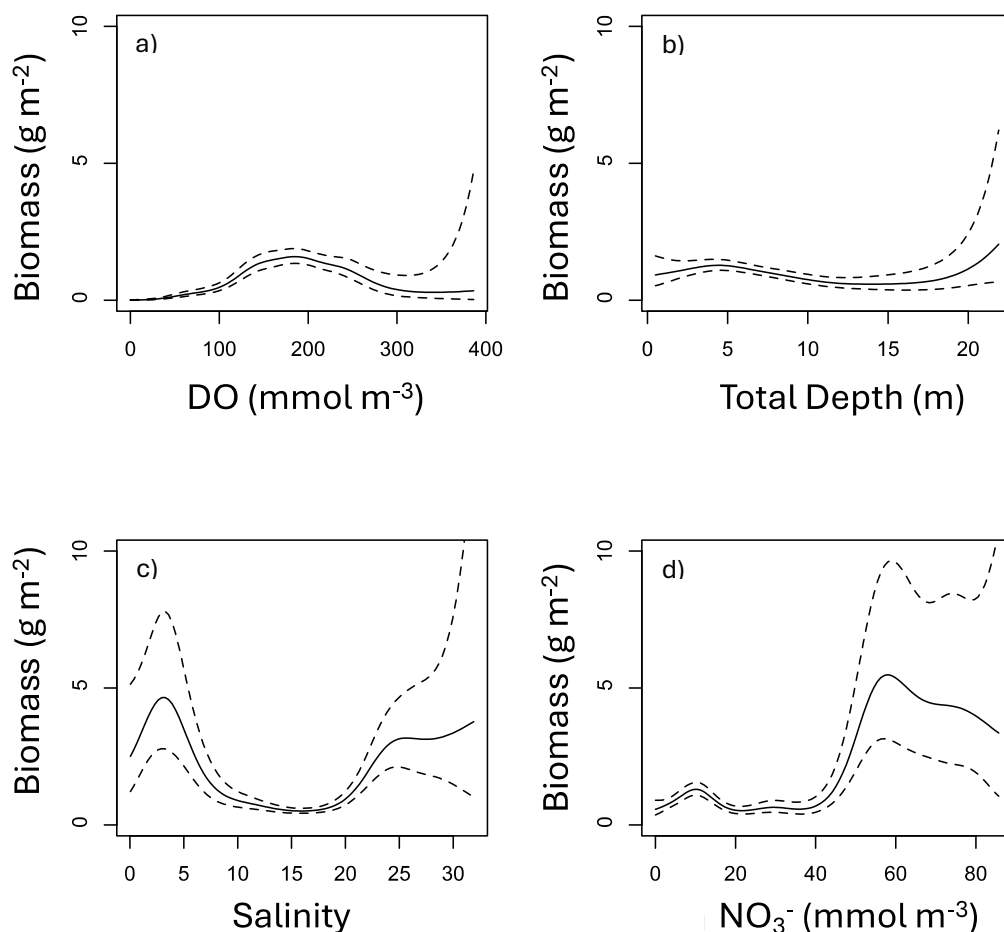
577

578

579

580

The relative effects of DO, salinity, NO_3^- and total depth on benthic biomass varied considerably. Figure 3 shows partial plots of the relative effect of these four significant predictor variables on total benthic biomass. Macrofauna biomass reaches its lowest values at low dissolved oxygen, the only section of all the partial plots that reach 0 g m^{-2} . Biomass is generally higher at shallower depths, although the effect is small. Biomass is highest at both low and high salinities and high surface NO_3^- . In summary, biomass is highest at moderate dissolved oxygen, shallow depths, low or high salinities, and high NO_3^- .



581

582 Figure 3: Partial plots of the effect of significant predictor variables on all-species biomass: (a)

583 bottom dissolved oxygen, (b) total depth, (c) bottom salinity, and (d) surface nitrate. Water

584 temperature and sand fraction were included in the model but omitted from display as they since

585 they did not significantly improve the model fit. The solid black line shows the response with the

586 dashed lines showing the 95% confidence interval. The natural log transformation was removed



587 from biomass to enhance viewing of the partial plots. The x-axis was cut-off at the upper quartile
588 plus three interquartile ranges in order to remove extreme outliers from the plots.

589

590 The model fit evaluation reveals some systemic biases examined in Fig. A2. The
591 residuals (observed values minus model-fitted values) are slightly skewed to the left (Fig. A2b),
592 meaning the model is more likely to overestimate biomass. The response vs. fitted value scatter
593 plot shows a nearly linear relationship (Fig. A2a). The map of residuals (Fig. A2c) shows that the
594 regions where the model is most likely to overestimate the biomass response are at the lowest
595 biomass zones in the Mid Bay and the lower Potomac River. In these sections, the biomass is
596 nearly zero. There is also an underestimation in the model fit at the high biomass zones,
597 especially in the Upper Bay.

598 ***3.3 Carbon flux estimates***

599 The biomass density and associated carbon fluxes vary across watershed regions, as
600 shown in Fig. A3. The associated carbon fluxes scale proportionally to the biomass with large
601 uncertainty. To evaluate our secondary production calculations, we examined the ratio of
602 secondary production to biomass. The ratio of the secondary production (in $\text{g C m}^{-2} \text{ yr}^{-1}$) to
603 biomass (in $\text{g m}^{-2} \text{ yr}^{-1}$) for the whole Bay was 1.6, with ratios ranging from 1.4 to 1.9 for the
604 different regions. Secondary production calculations from the two observationally validated
605 models, Dauer (1993), Edgar (1990), and Sturdivant et al., (2013) also found magnitudes within
606 that range.

607 In multiple segments of the Bay, respiration fluxes are comparable to the available
608 organic carbon supply. To assess the relative contribution of macrofaunal respiration, we
609 compared estimated respiration rates from benthic biomass to previously reported values for



610 primary production and other organic carbon inputs (Table 3). To estimate total organic carbon
611 (TOC) and particulate organic carbon (POC) fluxes in the Upper Bay, we calculated the areal
612 flux by distributing the total organic carbon load over the surface area of the tidal fresh and
613 oligohaline zones of the mainstem, represented by the CBP segments CB1 and CB2. This
614 approach assumes that the majority of the annual TOC load from the Susquehanna River remains
615 concentrated in the Upper Bay and is respired rather than transported downstream, an assumption
616 supported by Canuel & Hardison, (2016). In the Upper Bay, benthic macrofaunal respiration
617 fluxes are within the range of gross primary production (GPP). To estimate the fraction of
618 organic carbon load respired, we took the extreme ends of the uncertainty ranges of our
619 respiration rates and divided them by the sum of the estimates of GPP and POC in the Upper
620 Bay. The results suggest that 17 to 50% of available carbon in the Upper Bay is respired by
621 benthic macrofauna. Potomac River respiration rates exceed organic carbon production from
622 GPP. However, in the mainstem and the Bay as a whole, respiration fluxes are much lower than
623 GPP. Our estimates suggest that benthic macrofauna respire between 1.8 and 5.0% of the
624 available organic carbon in the mainstem.

625

626 Table 3: Primary production organic carbon, and respiration compiled from the listed studies
627 compared with respiration from our study. All units were converted to $\text{g C m}^{-2} \text{ yr}^{-1}$. The
628 watershed region areas were determined by summing the areas of the Chesapeake Bay Program
629 segments within each watershed. The Susquehanna River estimates assumed the entire load was
630 concentrated in the Upper Bay.

631



Region	Carbon Flux	Value	Study	Region (our study)	Carbon Flux (our study)	Value (our study)
Eastern North America	Estuarine GPP	309 g C m ⁻² yr ⁻¹	Najjar et al., (2018)	Whole Bay	Respiration	25±12 g C m ⁻² yr ⁻¹
Mid Atlantic Blight	TOC from tidal wetlands	6.8 g C m ⁻² yr ⁻¹	Herrmann et al., 2015			
Mid Atlantic Blight	TOC from streamflow	14.4 g C m ⁻² yr ⁻¹	Herrmann et al, 2015			
Mainstem	GPP	657.4 g C m ⁻² yr ⁻¹	Kemp et al., 1997	Mainstem	Respiration	23±11 g C m ⁻² yr ⁻¹
	Benthic Respiration	163.1 g C m ⁻² yr ⁻¹	Kemp et al., 1997			
All Inputs	TOC	90 g C m ⁻² yr ⁻¹	Kemp et al., 1997			
	POC	15.6 g C m ⁻² yr ⁻¹	Zhang & Blomquist (2018)			



Upper Bay	GPP	123.4 g C m ⁻² yr ⁻¹	Kemp et al., 1997	Upper Bay	Respiration	128±63 g C m ⁻² yr ⁻¹
	Benthic Respiration	44.3 g C m ⁻² yr ⁻¹	Kemp et al., 1997			
Susquehanna River	TOC	354 g C m ⁻² yr ⁻¹	Kemp et al., 1997			
	POC	257.7 g C m ⁻² yr ⁻¹	Zhang & Blomquist (2018)			
Potomac River	POC	31.7 g C m ⁻² yr ⁻¹	Zhang & Blomquist (2018)	Potomac	Respiration	57±29 g C m ⁻² yr ⁻¹

632

633 Benthic macrofaunal calcification also represents a major flux within the Bay. Our study
634 shows that calcification rates by benthic macrofauna analyzed in the BMP program far exceeds
635 estimates of the Eastern oyster (*Crassostrea virginica*) calcification rates (Table 4). To calculate
636 oyster calcification rates, we used Fulford et al., (2007) model estimates of oyster biomass in
637 different CBP segments and we related the ash-free dry weight of oyster biomass to the live
638 weight using a ratio of 10:1 (Mo & Neilson, 1994). We then calculated calcification rates using a
639 ratio of 2 mg CaCO₃ per gram live mass per day of oyster (Waldbusser et al., 2013). To maintain
640 consistency with our results, which frame fluxes in the context of carbon, we converted
641 calcification rates to the equivalent amount of CO₂ generated. While this is a non-standard way



of presenting calcification rates, it allows for direct comparison with other carbon fluxes and better integration into our broader analysis of estuarine carbon cycling. We estimated CO_2 generated (in $\text{g m}^{-2} \text{yr}^{-1}$) is about 12% of the CaCO_3 production (in $\text{g m}^{-2} \text{yr}^{-1}$) (Chauvaud et al., 2003). Using these values and CBP segment areas, we derived oyster calcification fluxes for the mainstem and Upper Bay. Remarkably, bivalve calcification rates from our study exceeds oyster calcification rates by over 80 times in the mainstem and by over 1000 times in the Upper Bay.

648

Table 4: Oyster calcification and riverine calcium input compiled from the listed studies compared with calcification from our study. Calcification calculated from the yearly Ca flux and oyster calcification from the listed studies. All units were converted to $\text{g C m}^{-2} \text{yr}^{-1}$ with information about how the calculations were made in the text. The watershed region areas were determined by summing the areas of the Chesapeake Bay Program segments within each watershed. The Upper Bay calcification from yearly Ca flux assumed that the entire load from the Susquehanna River was concentrated in the Upper Bay.

Region	Carbon Flux	Value	Study	Region (our study)	Carbon Flux (our study)	Value (our study)
Mainstem	Oyster Calcification	$0.17 \text{ g C m}^{-2} \text{yr}^{-1}$	Fulford et al., 2007/ Waldbusser et al., 2013	Mainstem	Calcification	$14 \pm 5 \text{ g C m}^{-2} \text{yr}^{-1}$



Upper Bay	Calcification from Yearly Ca Flux	557.6 g C m ⁻² yr ⁻¹	USGS	Upper Bay	Calcification	78±31 g C m ⁻² yr ⁻¹
	Oyster Calcification	0.07 g C m ⁻² yr ⁻¹	Fulford et al., 2007/ Waldbusser et al., 2013			
Potomac River	Calcification from Yearly Ca Flux	77.9 g C m ⁻² yr ⁻¹	USGS	Potomac	Calcification	35± 14 g C m ⁻² yr ⁻¹

656

657 Evaluating the role of bivalve calcification in utilizing calcium further underscores its
658 biogeochemical significance. If all the calcium used in bivalve calcification were sourced from
659 rivers, bivalves would consume a significant fraction of the available calcium (Table 4). To
660 quantify riverine calcium input, we used data from non-tidal USGS stations in the Susquehanna
661 and Potomac Rivers from 1995 to 2022. Annual calcium fluxes were calculated using Weighted
662 Regression on Time, Discharge, and Season (WRTDS; Hirsch et al., 2010). In calcification, one
663 mole of CaCO₃ is produced for every mole of Ca consumed. To keep units consistent, we again
664 estimated the CO₂ produced (in g m⁻² yr⁻¹) from 12% of the CaCO₃ production (in g m⁻² yr⁻¹).
665 The Upper Bay calculation assesses how much CO₂ bivalves would generate if all the
666 Susquehanna calcium input was used in calcification within the Upper Bay. Similarly, the
667 Potomac River calculation estimates the rates of calcification that would occur if all of the
668 calcium input into the Potomac River was utilized for calcification within the Potomac River.



669 Relative to annual riverine calcium fluxes, benthic macrofauna would use ~14% of the available
670 calcium in the Upper Bay and 45% in the Potomac River.

671 The role of benthic macrofaunal metabolic processes in the carbon budget is particularly
672 pronounced when the effects of calcification and respiration are combined. Our estimates
673 indicate that calcification contributes 38% of the total CO₂ flux while respiration accounts for
674 62% (Table 5). This combined CO₂ flux exceeds the amount of outgassing estimated in the
675 Upper Bay and the mainstem overall (Table 5). Compared to other estuaries worldwide, the
676 Chesapeake Bay exhibits relatively modest levels of CO₂ outgassing (Table 5). In estuaries with
677 greater outgassing rates, the proportional contribution of calcification and respiration to total
678 CO₂ exchange might be lower, but would still be substantial.

679
680 Table 5: Air/sea gas exchange from the listed studies compared with total benthic CO₂ flux in
681 our study, calculated as the sum of respiration and calcification fluxes. All units were converted
682 to g C m⁻² yr⁻¹.

Region	Carbon Flux	Value	Study	Region (our study)	Carbon Flux (our study)	Value (our study)
Upper Bay (CB1,	Air/Sea CO ₂ exchange	74.5 g C m ⁻² yr ⁻¹ (outgassing)	Herrmann et al., 2020	Upper Bay (CB1 & CB2)	Total CO ₂ Flux	205±70 g C m ⁻² yr ⁻¹



CB2, & CB3)						
Mainstem	Air/Sea CO ₂ exchange	14.5 g C m ⁻² yr ⁻¹ (outgassing)	Herrmann et al., 2020	Mainstem	Total CO ₂ Flux	36±12 g C m ⁻² yr ⁻¹
Global Estuaries	Air/Sea CO ₂ exchange	92.5 g C m ⁻² yr ⁻¹ (outgassing)	Chen et al., 2013	Whole Bay	Total CO ₂ Flux	40±14 g C m ⁻² yr ⁻¹
Eastern North America	Air/Sea CO ₂ exchange	108.1 g C m ⁻² yr ⁻¹ (outgassing)	Chen et al., 2013	Whole Bay		

683

684 4. Discussion

685 4.1. Environmental controls on benthic biomass distribution

686 Bivalve species distribution within the Bay is primarily driven by salinity tolerances.

687 Both the GAMs analysis (Table 2) and the biomass densities associated with salinity zones (Fig.

688 2) showed that benthic biomass, dominated by bivalves, was much higher at lower salinities. The

689 strong influence of salinity on benthic fauna distribution within estuaries has long been

690 recognized (Cain, 1975; Hopkins et al., 1973). This relationship is illustrated in our study by the

691 preference of the most abundant species, *R. Cuneata*, *L. balthica*, and *C. fluminea*, for less saline

692 water. *R. Cuneata* is widely known to need less saline waters, optimally between 1 and 15 ppt, to

693 survive (Hopkins et al., 1973). *C. fluminea* prefers freshwater environments (Phelps, 1994; Sousa



694 et al., 2008). *L. balthica* has a range of tolerances but abundance declines below 5 ppt (Jansson et
695 al., 2015). In our study, *L. balthica* is more concentrated between 5 and 13 ppt. While salinity
696 determines which species dominate, other factors influence their relative abundances within
697 these zones.

698 Within mesohaline zones, summer hypoxia appears to be driving extremely low benthic
699 biomass. In our GAMs analysis, an association existed between biomass and extremely low
700 bottom dissolved oxygen values. Among the different salinity zones, low biomass is associated
701 with low dissolved oxygen in the high mesohaline, where we had the lowest biomass densities.
702 Long-term exposure to hypoxia ($<2 \text{ mg L}^{-1}$ or 62.5 mmol m^{-3}) is fatal to benthic fauna (Diaz et
703 al., 1995; Seitz et al., 2006; Seitz et al., 2009) and many benthic communities (approximately
704 50%) only recover on an annual timescale (Diaz et al., 1995). In other words, regions that suffer
705 frequent hypoxia often see lower levels of benthic biomass even when hypoxic conditions are not
706 occurring. In the Chesapeake Bay, hypoxia is most likely to occur in the deeper, mesohaline
707 regions (Frankel et al., 2022; Zheng & DiGiacomo, 2020), providing evidence that our
708 suppressed values of benthic fauna at this salinity zone could be due to mass mortality from
709 hypoxia. This pattern is particularly evident where biomass is extremely low through the Mid
710 Bay and lower Potomac, regions typically associated with summer hypoxia (Sturdivant et al.,
711 2013).

712 Across the Bay, the relatively narrow range of summer bottom water temperatures likely
713 explains why temperature has an insignificant effect on the spatial distribution of benthic
714 biomass. In our GAMs analysis, summer bottom water temperature was not significantly
715 correlated with benthic biomass. Water temperature has been considered an important driver of
716 benthic biomass (Marsh & Tenore, 1990; Seitz et al., 2006; Seitz et al., 2009; Testa et al., 2020),



717 with low temperature specifically creating mass mortality of *R. cuneata* during winter and spring
718 (Tuszer-Kunc et al., 2020). Higher temperatures, however, will drive early and larger seasonal
719 hypoxia in the Chesapeake Bay (Hinson et al., 2022; Irby et al., 2018; Ni et al., 2019). So,
720 temperature could still indirectly affect benthic biomass through its effect on dissolved oxygen.
721 Therefore, while temperature may not directly drive spatial patterns of biomass, it could be
722 more relevant to temporal changes in biomass.

723 Although NO_3^- is a clear predictor of benthic biomass, the mechanisms driving this
724 association are likely complex. NO_3^- is an important limiting nutrient for primary production,
725 and high annually-averaged concentrations indicate an excess of NO_3^- not fully utilized by
726 phytoplankton. Excess NO_3^- from the tributaries flows into the mainstem, fueling a spring
727 phytoplankton bloom (Brush et al., 2020b). The highest primary production zones in the spring
728 are in the mesohaline and fuel hypoxia where the Bay is deeper and stratified (Brush et al.,
729 2020a), possibly explaining why long-term increases in phytoplankton biomass have not been
730 linked with an increase in benthic biomass (Harding & Perry, 1997). In the tidal fresh and
731 oligohaline zones, abundant NO_3^- is present, but high suspended solid loads limit light
732 penetration, consequently inhibiting primary production (Brush et al., 2020b).

733 Given the complexity of explaining the relationship between NO_3^- and benthic biomass,
734 further insights may come from examining the relationship between inorganic suspended solid
735 loads and POC. A significant portion of suspended solids in the tidal fresh and oligohaline
736 regions is POC, given previous studies have that suggest substantial inputs of POC are respired
737 in the Upper Bay (Kemp et al., 1997; Testa et al., 2020). Canuel & Hardison, (2016) further
738 demonstrated that above the Estuarine Turbidity Maximum (ETM), organic matter is dominated
739 by allochthonous (terrigenous) sources, which could contribute to the high POC content in



740 suspended solids. Further evidence for substantial allochthonous inputs of POC comes from the
741 dissolved oxygen supersaturation ($\Delta[\text{O}_2]$) model-derived information (Fig. 4). As explained
742 earlier, $\Delta[\text{O}_2]$ was not included as a predictor variable because it was highly correlated with
743 NO_3^- and salinity, the two most influential predictors of the high biomass zones. Under steady-
744 state conditions and ignoring advection and mixing, negative surface $\Delta[\text{O}_2]$ indicates net
745 heterotrophy, where oxygen consumption from respiration exceeds oxygen production from
746 photosynthesis. This imbalance leads to undersaturation and uptake from the atmosphere.
747 Conversely, positive $\Delta[\text{O}_2]$ indicates net autotrophy, where oxygen production from
748 photosynthesis exceeds oxygen consumption from respiration. The $\Delta[\text{O}_2]$ maps (Fig. 4) indicate
749 high levels of heterotrophy year-round throughout the upper reaches of the tributaries and the
750 Upper Bay, corresponding to the tidal fresh and oligohaline zones of the Bay. Autotrophy
751 dominates year-round in the polyhaline Lower Bay. In the lower tributaries and Mid Bay
752 (mesohaline zones), there are seasonal shifts, with heterotrophy in the summer and fall and
753 autotrophy in the spring and winter. High levels of heterotrophy near the freshwater sources of
754 the Bay could indicate substantial inputs of allochthonous organic matter being respired (Kemp
755 et al., 1997).

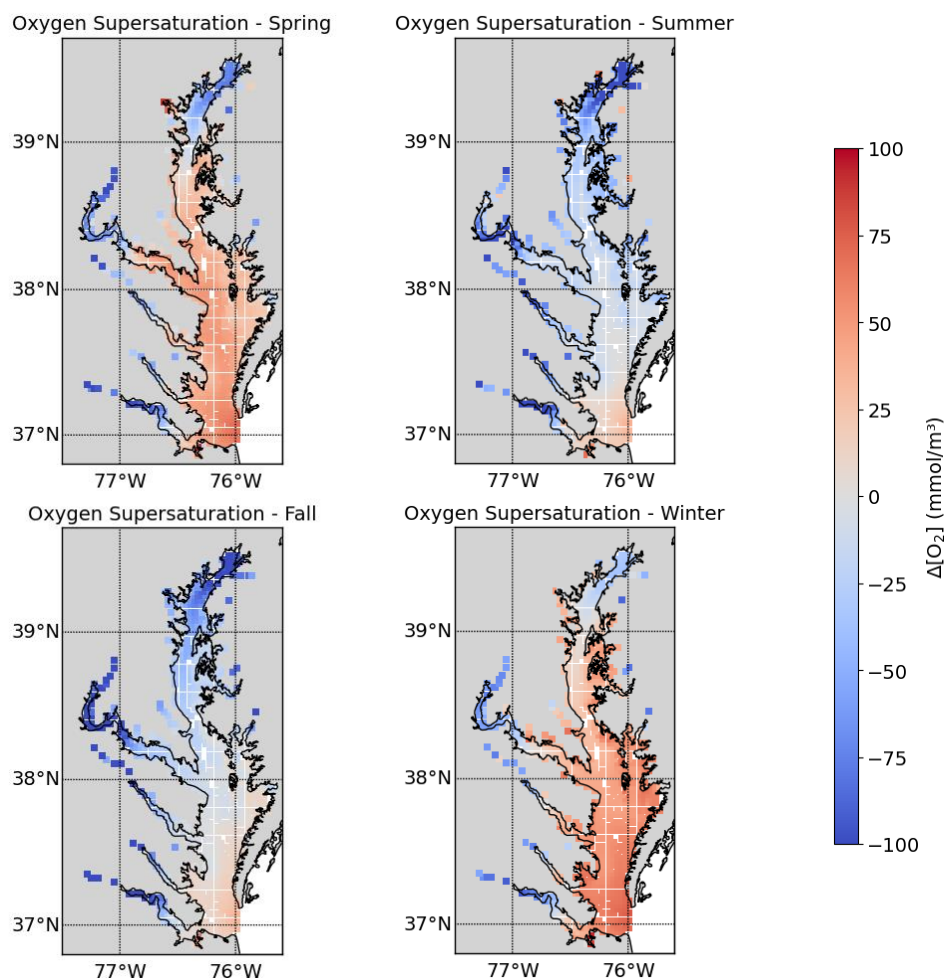


Figure 4: Surface oxygen supersaturation for each season in the Bay. Spring (March–April), Summer (July–August), Fall (September–November), and Winter (December–February). Method for calculating oxygen supersaturation is described in the text.

If the highest NO_3^- concentrations coincide with elevated suspended solid loads at and above the ETM, and if POC is substantially present in these loads, then annually averaged NO_3^- may act as a proxy for allochthonous POC. In contrast, below the ETM, NO_3^- is more readily



utilized in primary production, and most of the POC is autochthonous. Unfortunately, POC modeled by ROMS-ECB can't be used to support our hypothesis, as model-data evaluation did not meet our robustness threshold ($r_s < 0.7$). However, USGS data compiled by Zhang & Blomquist (2018) give long-term averages (1985–2016) of POC input into various tributaries measured at non-tidal gauging stations. Figure 5 compares the concentration of allochthonous input of POC and the average surface nitrate NO_3^- in each tidal region. We calculated the POC concentration using the average load of POC input into the tributary divided by the area of the watershed region. Only the six largest tributaries had POC data reported. The Susquehanna River data was excluded because it discharges directly into the mainstem, making it less comparable to the other river estuaries. There was a substantial linear correlation between NO_3^- and POC.

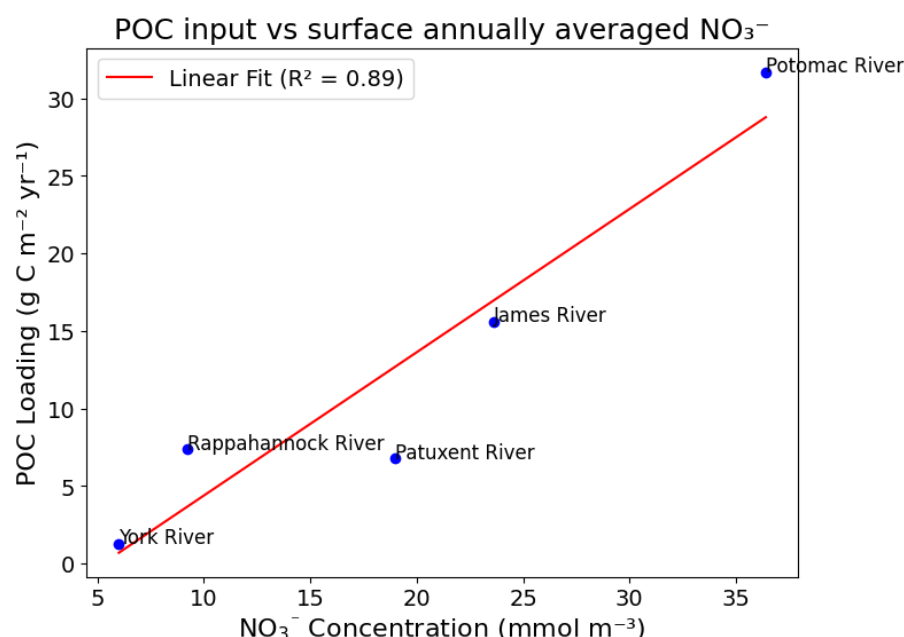


Figure 5: Particulate organic carbon (POC) vs surface nitrate (NO_3^-) for five watershed regions. POC fluxes were calculated using load data from USGS compiled by Zhang and Blomquist



(2018). The watershed region areas were determined by summing the areas of the Chesapeake Bay Program segments within each watershed. NO_3^- concentrations were obtained from ROMS-ECB output and represent the annually averaged mean concentration in each watershed region.

Taken together, these data strongly support the hypothesis that the correlation between surface NO_3^- and benthic biomass is driven by allochthonous POC. This link is further reinforced by our dataset, where regions of high heterotrophy (Fig. 4) align with the highest benthic biomass (Fig. 1). If salinity dictates species distribution by limiting certain taxa to fresher zones and dissolved oxygen reduces benthic biomass in mesohaline zones, then the relative inputs of terrestrial organic matter could be controlling biomass variation in the fresher regions.

4.2. Benthic macrofaunal contributions to estuarine carbon budget

The higher benthic biomass in less saline waters suggests a significant role for respiration in the carbon budget in this region. The proportion of organic carbon respired by benthic macrofauna estimated in our study in the Upper Bay (17 to 50%) is remarkably similar to the 14 to 40% range estimated for bivalve filter feeders in tidal fresh and oligohaline waters by Cerco & Noel (2010). In the Upper Bay, where the benthic macrofauna respiration flux is comparable to the GPP flux, if all the GPP were respired solely by benthic macrofauna, net ecosystem production would be zero. However, given the consideration of additional respiration by other organisms (e.g., microbes and pelagic zooplankton) the allochthonous POC from the Susquehanna River must be a critical source of organic carbon driving net heterotrophy in this region. These findings reinforce the earlier conclusion that high biomass zones in the Upper Bay are sustained by allochthonous organic inputs. The Potomac River, however, presents a less conclusive case, partly due to the lack of available GPP estimates. In the Potomac, where benthic



801 macrofaunal respiration rates exceed the estimated POC flux, additional carbon sources, such as
802 autochthonous GPP or tidal wetland outwelling, may be contributing to carbon metabolism.
803 Herrmann et al., (2015) estimated that wetland outwelling accounts for approximately half of the
804 organic carbon exported by streamflow in Mid-Atlantic estuaries.

805 Benthic macrofaunal respiration plays a smaller role in the rest of the Bay, where
806 autochthonous organic carbon dominates. For both the mainstem and the whole Bay, the
807 estimated primary production far exceeds the average estimated respiration rates calculated from
808 our benthic biomass data. Overall, the autochthonous organic carbon contribution from primary
809 production is about 15 times greater than the allochthonous input from estuaries in the Mid-
810 Atlantic Bight. This ratio is even more pronounced since only a fraction of the total organic
811 carbon (TOC) is particulate (POC) and can be respired by the benthos (Kemp et al., 1997). Kemp
812 et al., (1997) calculated benthic respiration from sulfate reduction and sediment oxygen
813 consumption rates. Their estimates could highlight the relatively modest role of benthic
814 macrofaunal respiration for the entire mainstem, given the lower biomass values in the Mid and
815 Lower Bay, where autochthonous primary production and overall organic carbon flux to the
816 sediments are higher. Their calculation may have underestimated benthic respiration rates, as our
817 respiration rates estimates for benthic macrofaunal respiration are higher than their calculations.
818 Our estimates of benthic macrofaunal respiration in the mainstem (1.8–5.0%) is significantly
819 lower than estimates derived from the combined findings of Hopkinson & Smith, (2004) and
820 Rodil et al., (2022). Hopkinson & Smith, (2004) estimated that approximately 24% of organic
821 carbon is respired by the benthos, while Rodil et al., (2022) found that benthic macrofauna
822 account for roughly 40% of total benthic respiration. Taken together, these studies suggest that
823 around 10% of available organic carbon is expected to be respired by benthic macrofauna, more



824 than double our findings. Although our estimates indicate that benthic macrofaunal respiration
825 accounts for a relatively small fraction of total organic carbon metabolism at the scale of the
826 entire Bay, this does not preclude the existence of localized hotspots where it plays a dominant
827 role.

828 Unlike the extensive research on estuarine benthic respiration, little attention has been
829 given to calcification, yet our findings suggest that benthic macrofaunal calcification could be
830 important to the carbon budget. The relative importance of bivalve calcification in the Bay is
831 illustrated in Table 4. Eastern oysters (*Crassostrea virginica*) have received significant attention
832 due to their ecological and economic importance, but their populations in the Chesapeake Bay
833 used to be at least two orders of magnitude higher than its present levels (Fulford et al., 2007;
834 Newell, 1988). The bivalves sampled in the BMP program contribute substantially more to
835 estuarine carbon cycling than present-day Eastern populations. Evaluating the role of bivalve
836 calcification in utilizing calcium further underscores its biogeochemical significance. Our
837 estimations assume that all calcium input is used in calcification; however, since calcium
838 contributions from the ocean and groundwater may far exceed riverine inputs, this comparison
839 does not represent a complete calcium budget but rather provides a useful context for
840 understanding the scale of bivalve calcification.

841 Benthic macrofauna may play a major role in CO₂ outgassing, as indicated by our
842 estimated high carbon fluxes in the Upper Bay and upper tributaries relative to air-sea gas
843 exchange. Furthermore, our total CO₂ generation estimates for the Upper Bay ($205 \pm 70 \text{ g C m}^{-2}$
844 yr^{-1}), where bivalve biomass is concentrated, exceed those reported by Chauvaud et al., (2003),
845 who estimated CO₂ production from calcification and respiration at $55 \pm 51 \text{ g C m}^{-2} \text{ yr}^{-1}$ for the
846 bivalve *P. amurensis* in Northern San Francisco Bay. This further supports their hypothesis that



847 benthic calcifiers can serve as major CO₂ generators in estuaries. Given the high heterotrophy in
848 the Upper Bay and upper tributaries, as well as the balance between benthic macrofaunal
849 respiration and organic carbon inputs in the Potomac River, it is conceivable that benthic
850 macrofauna are major contributors to CO₂ outgassing in these regions.

851 **Conclusion**

852 This study examines how water chemistry and sediment composition influence the
853 spatial distribution of benthic biomass and to assess the role macrofaunal respiration and
854 calcification plays in estuarine carbon budgets. We found that benthic macrofauna, especially
855 bivalves, were concentrated in the upper portions of the tributaries and mainstem Bay. High
856 biomass zones generally had low salinity, high surface NO₃⁻, moderate dissolved oxygen, and
857 low depth. NO₃⁻ could behave as a proxy for POC, with high biomass being driven by
858 allochthonous POC in the tidal fresh and oligohaline zones, areas with lower autochthonous
859 primary production and high heterotrophy. Calcification from benthic macrofauna biomass could
860 be a significant sink of calcium in the Bay, and the calcification rates from bivalves collected in
861 the BMP program far exceeds Eastern oyster calcification rates. CO₂ generated from
862 calcification and respiration could substantially contribute to outgassing in the tidal fresh and
863 oligohaline zones. These findings highlight the significant role of benthic macrofauna in
864 estuarine biogeochemical cycling, particularly in Chesapeake Bay.

865 Estuarine numerical models have historically focused on microbiota while overlooking
866 the role of macrobiota in biogeochemical transformations (Ehrnsten et al., 2020; Ganju et al.,
867 2016). However, our study demonstrates that benthic macrofauna can significantly influence
868 carbon dynamics within the Chesapeake Bay and should be more consistently incorporated into
869 numerical models. Additionally, we show that the spatial distribution of benthic macrofauna is



870 highly predictable based on environmental variables already included in models, reducing the
871 need for high-resolution benthic biomass data. Our findings provide a strong foundation for
872 integrating benthic macrofauna into numerical models, highlight both the feasibility and
873 necessity of doing so.

874 Several limitations in our study must also be acknowledged. One key limitation is the
875 need for better empirical equations relating biomass to metabolic processes, particularly
876 calcification. Our estimates relied heavily on Chauvaud et al., (2003), who assumes a direct
877 proportionality between secondary production rates and calcification rates, but this relationship
878 requires further validation across different estuarine systems. However, we attempted to account
879 for this uncertainty by incorporating a range of estimates in our analysis. Additionally, our study
880 was constrained by the interactions between highly correlated variables. As a result, we did not
881 use our calculated values for Ω_{arag} , despite its potential importance for bivalves. The saturation
882 state of aragonite could strongly influence calcification rates, but due to its correlation with other
883 environmental variables, its independent effect was difficult to parse. Furthermore, while our
884 model explained a little over half of the deviance in biomass from predictor variables, this
885 predictive capability could be improved. In our study we emphasized bottom-up controls. Top-
886 down controls such as predation could also play a significant role in biomass distributions.

887 Future research should focus on refining metabolic estimates and further investigating the
888 factors driving temporal changes in biomass. Climate change, along with ongoing management
889 efforts aimed at reducing nutrient loading, is expected to alter key water quality parameters.
890 Understanding how these shifts will impact benthic biomass distribution and metabolism is
891 critical for predicting their broader impacts on ecosystem functioning and biogeochemical
892 cycling.



893 Overall, our findings emphasize the predictability of benthic biomass distributions within
894 estuaries and their importance to estuarine carbon budgets, underscoring their need for further
895 integration into numerical models.

896

897

898

899

900

901

902

903

904

905

906

907

908

909

910

911

912

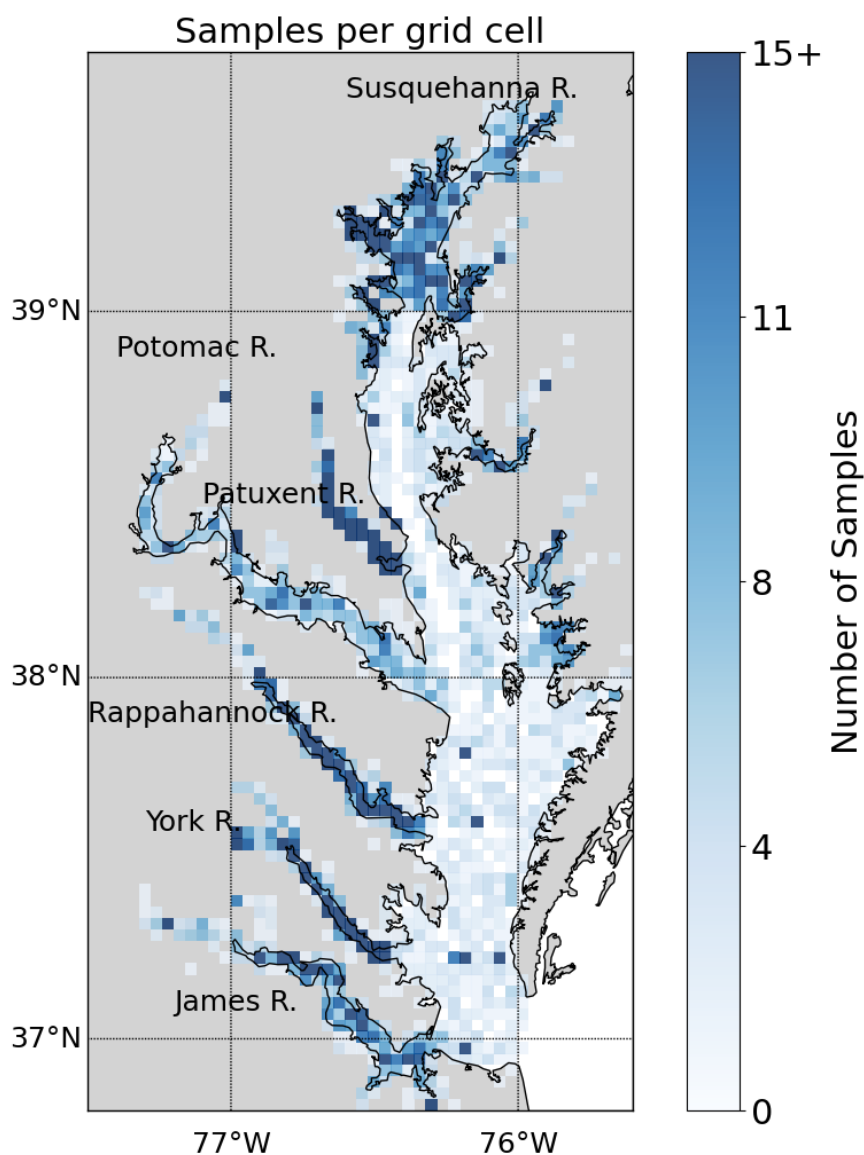
913

914

915



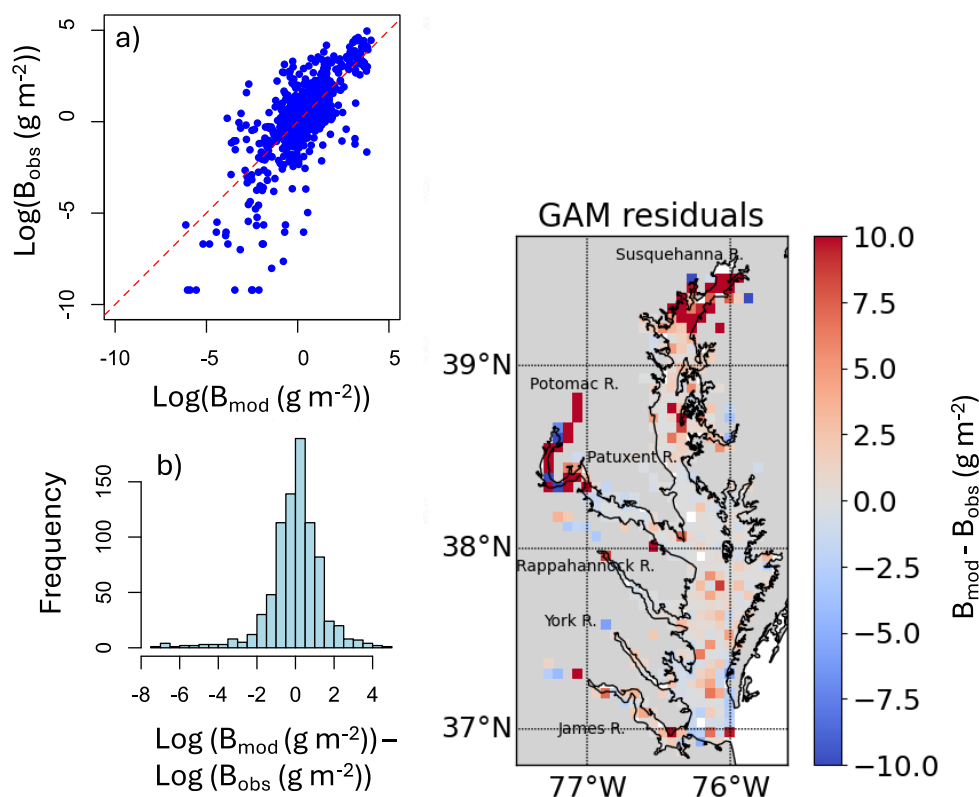
916 **Appendix A**



917

918 Figure A1: Number of benthic samples collected in each grid cell in the summer (July 15 to
919 September 30) from 1995 to 2022 from the Maryland and Virginia Benthic Monitoring Program.

920 The grids are approximately square, measuring 3.5 km by 3.5 km. Each grid cell contains a time-
921 average of each measurement collected in the cell



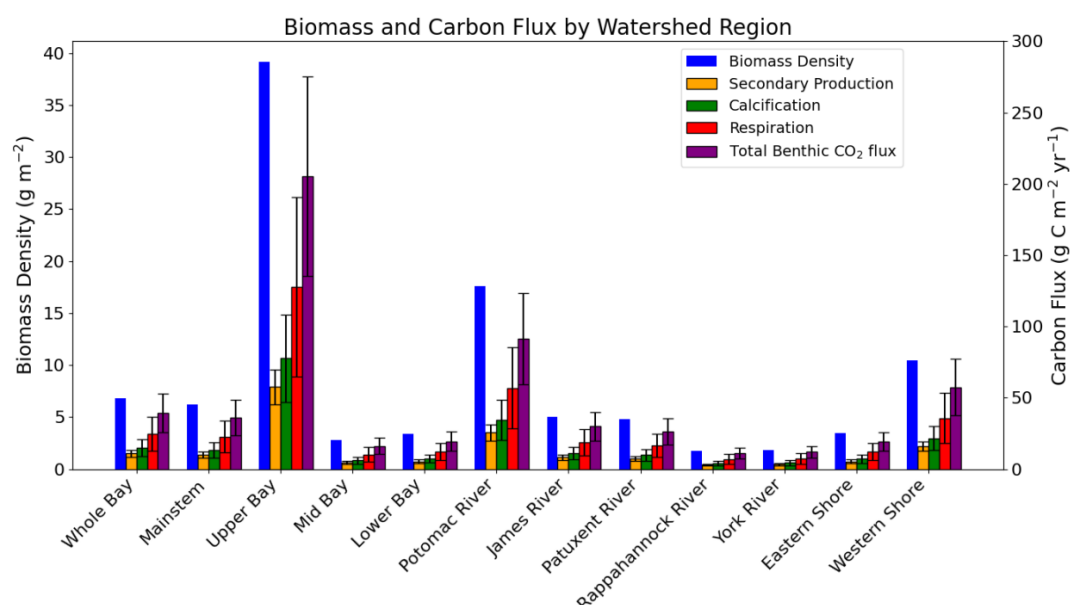
922

923 Figure A2: Evaluation of the total biomass GAM, which includes DO, salinity, total depth, , and

924 NO_3^- , sand fraction, and water temperature as predictor variables. “Log” refers to the natural

925 logarithm. (a) Modeled vs. observed values. (b) Histogram of biomass residuals (modeled minus

926 observed values, $B_{\text{mod}} - B_{\text{obs}}$). (c) Spatial distribution of the residuals.



927

928 Figure A3: Biomass density and carbon fluxes for each watershed region in the Bay. The carbon
 929 fluxes are the mean value with associated total uncertainty range, as described in the text.

930

931 Data Availability

932 All data used in this study are publicly available and have been described in the Methods section.

933 Water quality data were obtained from the *Chesapeake Bay Water Quality Monitoring Program*

934 (<https://datahub.chesapeakebay.net/WaterQuality>), and benthic data were sourced from the

935 *Chesapeake Bay Long-Term Benthic Monitoring Program*

936 (<https://www.baybenthos.versar.com/data.htm>). Model output used in this study is publicly

937 available at <https://www.seanoe.org/data/00882/99441/>.

938

939 Author Contribution



940 SA led the research, conducted data analysis, interpreted results, and wrote the initial and
941 subsequent drafts of the manuscript.

942 RN conceptualized the project, defined overarching research goals, secured financial support,
943 and contributed substantially to manuscript drafts through critical reviews, commentary, and
944 revisions.

945 ER provided significant insights from her expertise on the physiological responses of marine
946 invertebrates to environmental variables, influencing the scope and direction of the study. She
947 also substantially contributed to manuscript revisions through critical reviews and commentary.

948 RW contributed significant expertise on benthic biomass distribution in Chesapeake Bay and
949 generalized additive modeling techniques, shaping the analytical framework of the study. He
950 provided critical feedback and revisions during manuscript preparation.

951 MF provided ongoing feedback throughout the research process, particularly regarding the
952 integration of modeling information and interpretation of results, and contributed critical
953 commentary on multiple presentations of the work.

954 PS consistently provided feedback and contributed modeling expertise, assisting with data
955 interpretation and manuscript revisions through critical reviews and commentary.

956 SD developed the original empirical models linking benthic macrofaunal biomass to carbon
957 fluxes, laying foundational methodological contributions to the study.

958

959 **Competing Interests**

960 The authors declare that they have no conflict of interest.

961

962 **Acknowledgements**



963 We thank Maria Herrmann, Jill Arriola, and Alexa Labossiere for their valuable discussions and
964 feedback that contributed to this manuscript. We also acknowledge Riley Westman and Edward
965 Stets for providing riverine calcium input data from the USGS. Additionally, we used AI tools,
966 including Grammarly and ChatGPT, to assist with grammar and clarity in sentence editing.

967

968 **Financial Support**

969 This work is supported by the National Science Foundation (NSF) Chemical and Biological
970 Oceanography Program under Grant No. OCE-2148949 and the U.S. Department of Energy
971 (DOE) as part of the Integrated Coastal Modeling (ICoM) project.

972

973

974

975

976

977

978

979

980

981

982

983

984

985



986 References

- 987 Akoglu, H. (2018). User's guide to correlation coefficients. *Turkish Journal of Emergency*
988 *Medicine*, 18(3), 91–93. <https://doi.org/10.1016/j.tjem.2018.08.001>
- 989 Alden, R. W., Dauer, D. M., Ranasinghe, J. A., Scott, L. C., & Llansó, R. J. (2002). Statistical
990 verification of the Chesapeake Bay benthic index of biotic integrity. *Environmetrics: The*
991 *Official Journal of the International Environmetrics Society*, 13(5–6), 473–498.
992 <https://doi.org/10.1002/env.548>
- 993 Beckwith, S. T., Byrne, R. H., & Hallock, P. (2019). Riverine calcium end-members improve
994 coastal saturation state calculations and reveal regionally variable calcification potential.
995 *Frontiers in Marine Science*, 6(APR). <https://doi.org/10.3389/fmars.2019.00169>
- 996 Birchenough, S. N. R., Reiss, H., Degraer, S., Mieszkowska, N., Borja, Á., Buhl-Mortensen, L.,
997 Braeckman, U., Craeymeersch, J., De Mesel, I., Kerckhof, F., Kröncke, I., Parra, S., Rabaut,
998 M., Schröder, A., Van Colen, C., Van Hoey, G., Vincx, M., & Wätjen, K. (2015). Climate
999 change and marine benthos: a review of existing research and future directions in the North
1000 Atlantic. *Wiley Interdisciplinary Reviews: Climate Change*, 6(2), 203–223.
1001 <https://doi.org/10.1002/wcc.330>
- 1002 Borja, A., Dauer, D. M., Díaz, R., Llansó, R. J., Muxika, I., Rodríguez, J. G., & Schaffner, L.
1003 (2008). Assessing estuarine benthic quality conditions in Chesapeake Bay: a comparison of
1004 three indices. *Ecological Indicators*, 8(4), 395–403.
1005 <https://doi.org/10.1016/j.ecolind.2007.05.003>
- 1006 Brey, T. (1990). Confidence limits for secondary production estimates: application of the
1007 bootstrap to the increment summation method *. *Marine Biology*, 106, 503–508.
- 1008 Brush, M. J., Giani, M., Totti, C., Testa, J. M., Faganeli, J., Ogrinc, N., Michael Kemp, W., &
1009 Umani, S. F. (2020). Eutrophication, harmful algae, oxygen depletion, and acidification. In
1010 T. C. Malone, A. Malej, & J. Faganeli (Eds.), *Coastal ecosystems in transition: A*
1011 *comparative analysis of the Northern Adriatic and Chesapeake Bay* (pp. 75–104). Wiley.
1012 <https://doi.org/10.1002/9781119543626.ch5>
- 1013 Brush, M. J., Mozetič, P., Francé, J., Aubry, F. B., Djakovac, T., Faganeli, J., Harris, L. A., &
1014 Niesen, M. (2020). Phytoplankton dynamics in a changing environment. In T. C. Malone, A.
1015 Malej, & J. Faganeli (Eds.), *Coastal ecosystems in transition: A comparative analysis of the*
1016 *Northern Adriatic and Chesapeake Bay* (pp. 49–74). Wiley.
1017 <https://doi.org/10.1002/9781119543626.ch4>
- 1018 Cain, T. D. (1975). Reproduction and recruitment of the brackish water clam, *Rangia cuneata* in
1019 the James River, Virginia. *Fishery Bulletin*, 73(2), 412.
1020 <https://scholarworks.wm.edu/vimsarticles/2139>



- 1021 Canuel, E. A., & Hardison, A. K. (2016). Sources, ages, and alteration of organic matter in
1022 estuaries. *Annual Review of Marine Science*, 8, 409–434. [https://doi.org/10.1146/annurev-](https://doi.org/10.1146/annurev-marine-122414-034058)
1023 [marine-122414-034058](https://doi.org/10.1146/annurev-marine-122414-034058)
- 1024 Cerco, C. F., & Noel, M. R. (2010). Monitoring, modeling, and management impacts of bivalve
1025 filter feeders in the oligohaline and tidal fresh regions of the Chesapeake Bay system.
1026 *Ecological Modelling*, 221(7), 1054–1064. <https://doi.org/10.1016/j.ecolmodel.2009.07.024>
- 1027 Chauvaud, L., Thompson, J. K., Cloern, J. E., & Thouzeau, G. (2003). Clams as CO₂ generators:
1028 The *Potamocorbula amurensis* example in San Francisco Bay. *Limnology and*
1029 *Oceanography*, 48(6), 2086–2092. <https://doi.org/10.4319/lo.2003.48.6.2086>
- 1030 Chesapeake Bay Program. (n.d.). *CBP Water Quality Database (1984-present)*.
- 1031 Dauer, D. M. (1993). Biological criteria, environmental health and estuarine macrobenthic
1032 community structure. *Marine Pollution Bulletin*, 26(5), 249–257.
1033 [https://doi.org/10.1016/0025-326X\(93\)90063-P](https://doi.org/10.1016/0025-326X(93)90063-P)
- 1034 Dauer, D. M., & Alden III, R. W. (1995). Long-term trends in the macrobenthos and water
1035 quality of the lower Chesapeake Bay (1985-1991). *Marine Pollution Bulletin*, 30(12), 840–
1036 850.
- 1037 Dauer, D. M., & Lane, M. F. (2010). *Quality assurance/quality control plan: Benthic biological*
1038 *monitoring program of the Lower Chesapeake Bay (July 1, 2010 to June 30, 2011)*.
- 1039 Dauer, D. M., Ranasinghe, J. A., & Weisberg, S. B. (2000). Relationships between benthic
1040 community condition, water quality, sediment quality, nutrient loads, and land use patterns
1041 in Chesapeake Bay. *Estuaries*, 23(1), 80–96.
- 1042 Diaz, R. J., & Schaffner, L. C. (1990). *Perspectives on the Chesapeake Bay, 1990* (M. Haire & E.
1043 C. Krome, Eds.).
- 1044 Diaz, R., Rosenberg, R., D Ansell R N Gibson, C. A., Barnes, M., & Diaz, R. J. (1995). Marine
1045 benthic hypoxia: a review of its ecological effects and the behavioural responses of benthic
1046 macrofauna. *Oceanography and Marine Biology. An Annual Review*, 33, 245–303.
1047 <https://www.researchgate.net/publication/236628341>
- 1048 Dolbeth, M., Cusson, M., Sousa, R., & Pardal, M. A. (2012). Secondary production as a tool for
1049 better understanding of aquatic ecosystems. *Canadian Journal of Fisheries and Aquatic*
1050 *Sciences*, 69(7), 1230–1253. <https://doi.org/10.1139/F2012-050>
- 1051 Dormann, C. F., Elith, J., Bacher, S., Buchmann, C., Carl, G., Carré, G., García Marquéz, J. R.,
1052 Gruber, B., Lafourcade, B., Leitão, P. J., Münkemüller, T., McClean, C., Osborne, P. E.,
1053 Reineking, B., Schröder, B., Skidmore, A. K., Zurell, D., & Lautenbach, S. (2013).
1054 Collinearity: a review of methods to deal with it and a simulation study evaluating their
1055 performance. *Ecography*, 36(1), 27–46.



- 1056 Drexler, M., & Ainsworth, C. H. (2013). Generalized Additive Models Used to Predict Species
1057 Abundance in the Gulf of Mexico: An Ecosystem Modeling Tool. *PLoS ONE*, 8(5).
1058 <https://doi.org/10.1371/journal.pone.0064458>
- 1059 Edgar, G. J. (1990). The use of the size structure of benthic macrofaunal communities to estimate
1060 faunal biomass and secondary production. *Journal of Experimental Marine Biology and*
1061 *Ecology*, 137(3), 195–214.
- 1062 Ehrnsten, E., Norkko, A., Müller-Karulis, B., Gustafsson, E., & Gustafsson, B. G. (2020). The
1063 meagre future of benthic fauna in a coastal sea—Benthic responses to recovery from
1064 eutrophication in a changing climate. *Global Change Biology*, 26(4), 2235–2250.
1065 <https://doi.org/10.1111/gcb.15014>
- 1066 Ehrnsten, E., Norkko, A., Timmermann, K., & Gustafsson, B. G. (2019). Benthic-pelagic
1067 coupling in coastal seas – Modelling macrofaunal biomass and carbon processing in
1068 response to organic matter supply. *Journal of Marine Systems*, 196, 36–47.
1069 <https://doi.org/10.1016/j.jmarsys.2019.04.003>
- 1070 Frankel, L. T., Friedrichs, M. A. M., St-Laurent, P., Bever, A. J., Lipcius, R. N., Bhatt, G., &
1071 Shenk, G. W. (2022). Nitrogen reductions have decreased hypoxia in the Chesapeake Bay:
1072 Evidence from empirical and numerical modeling. *Science of the Total Environment*, 814.
1073 <https://doi.org/10.1016/j.scitotenv.2021.152722>
- 1074 Fujii, T., & Raffaelli, D. (2008). Sea-level rise, expected environmental changes, and responses
1075 of intertidal benthic macrofauna in the Humber estuary, UK. *Marine Ecology Progress*
1076 *Series*, 371, 23–35. <https://doi.org/10.3354/meps07652>
- 1077 Fulford, R. S., Breitburg, D. L., Newell, R. I. E., Kemp, W. M., & Luckenbach, M. (2007).
1078 Effects of oyster population restoration strategies on phytoplankton biomass in Chesapeake
1079 Bay: a flexible modeling approach. *Marine Ecology Progress Series*, 336, 43–1.
- 1080 Galimany, E., Lunt, J., Freeman, C. J., Houk, J., Sauvage, T., Santos, L., Lunt, J., Kolmakova,
1081 M., Mossop, M., Domingos, A., Phlips, E. J., & Paul, V. J. (2020). Bivalve feeding
1082 responses to microalgal bloom species in the Indian River Lagoon: the potential for top-
1083 down control. *Estuaries and Coasts*, 43(6), 1519–1532. [https://doi.org/10.1007/s12237-020-](https://doi.org/10.1007/s12237-020-00746-9)
1084 [00746-9](https://doi.org/10.1007/s12237-020-00746-9)
- 1085 Ganju, N. K., Brush, M. J., Rashleigh, B., Aretxabaleta, A. L., del Barrio, P., Gear, J. S., Harris,
1086 L. A., Lake, S. J., McCardell, G., O'Donnell, J., Ralston, D. K., Signell, R. P., Testa, J. M.,
1087 & Vaudrey, J. M. P. (2016). Progress and challenges in coupled hydrodynamic-ecological
1088 estuarine modeling. *Estuaries and Coasts*, 39(2), 311–332. [https://doi.org/10.1007/s12237-](https://doi.org/10.1007/s12237-015-0011-y)
1089 [015-0011-y](https://doi.org/10.1007/s12237-015-0011-y)



- 1090 Garcia, H. E., & Gordon, L. I. (1992). Oxygen solubility in seawater: Better fitting equations.
1091 *Limnology and Oceanography*, 37(6), 1307–1312.
1092 <https://doi.org/10.4319/lo.1992.37.6.1307>
- 1093 Grant, J., & Thorpe, B. (1991). Effects of suspended sediment on growth, respiration, and
1094 excretion of the soft-shell clam (*Mya arenaria*). *Canadian Journal of Fisheries and Aquatic*
1095 *Sciences*, 48(7).
- 1096 Grebmeier, J. M., Bluhm, B. A., Cooper, L. W., Denisenko, S. G., Iken, K., Kędra, M., &
1097 Serratos, C. (2015). Time-series benthic community composition and biomass and
1098 associated environmental characteristics in the Chukchi Sea during the RUSALCA 2004-
1099 2012 Program. *Oceanography*, 28(3), 116–133. <https://doi.org/10.2307/24861905>
- 1100 Grüss, A., Drexler, M., & Ainsworth, C. H. (2014). Using delta generalized additive models to
1101 produce distribution maps for spatially explicit ecosystem models. *Fisheries Research*, 159,
1102 11–24. <https://doi.org/10.1016/j.fishres.2014.05.005>
- 1103 Guisan, A., Edwards, T. C., & Hastie, T. (2002). Generalized linear and generalized additive
1104 models in studies of species distributions: setting the scene. *Ecological Modelling*, 157(2–
1105 3), 89. www.elsevier.com/locate/ecolmodel
- 1106 Hagy, J. D. (2002). *Eutrophication, hypoxia and trophic transfer efficiency in Chesapeake Bay*
1107 [Doctoral dissertation, University of Maryland, College Park].
1108 <https://www.researchgate.net/publication/237005296>
- 1109 Harding, L. W., & Perry, E. S. (1997). Long-term increase of phytoplankton biomass in
1110 Chesapeake Bay, 1950-1994. *Marine Ecology Progress Series*, 157, 39–52.
- 1111 Hartwell, S. I., Wright, D. A., Takacs, R., & Hocutt, C. H. (1991). Relative respiration and
1112 feeding rates of oyster and brackish water clam in variously contaminated waters. *Marine*
1113 *Pollution Bulletin*, 22(4), 191–197.
- 1114 Hastie, T., & Tibshirani, R. (1987). Generalized additive models: some applications. *Journal of*
1115 *the American Statistical Association*, 82(398).
- 1116 Hauke, J., & Kossowski, T. (2011). Comparison of values of Pearson's and Spearman's
1117 correlation coefficients on the same sets of data. *Quaestiones Geographicae*, 30(2), 87–93.
1118 <https://doi.org/10.2478/v10117-011-0021-1>
- 1119 Herrmann, M., Najjar, R. G., Da, F., Friedman, J. R., Friedrichs, M. A. M., Goldberger, S.,
1120 Menendez, A., Shadwick, E. H., Stets, E. G., & St-Laurent, P. (2020). Challenges in
1121 quantifying air-water carbon dioxide flux using estuarine water quality data: Case study for
1122 Chesapeake Bay. *Journal of Geophysical Research: Oceans*, 125(7).
1123 <https://doi.org/10.1029/2019JC015610>



- 1124 Herrmann, M., Najjar, R. G., Kemp, W. M., Alexander, R. B., Boyer, E. W., Cai, W. J., Griffith,
1125 P. C., Kroeger, K. D., McCallister, S. L., & Smith, R. A. (2015). Net ecosystem production
1126 and organic carbon balance of U.S. East Coast estuaries: A synthesis approach. *Global*
1127 *Biogeochemical Cycles*, 29(1), 96–111. <https://doi.org/10.1002/2013GB004736>
- 1128 Hinson, K. E., Friedrichs, M. A. M., St-Laurent, P., Da, F., & Najjar, R. G. (2022). Extent and
1129 causes of Chesapeake Bay warming. *Journal of the American Water Resources Association*,
1130 58(6), 805–825. <https://doi.org/10.1111/1752-1688.12916>
- 1131 Hirsch, R. M., Moyer, D. L., & Archfield, S. A. (2010). Weighted regressions on time, discharge,
1132 and season (WRTDS), with an application to Chesapeake Bay river inputs. *Journal of the*
1133 *American Water Resources Association*, 46(5), 857–880. [https://doi.org/10.1111/j.1752-](https://doi.org/10.1111/j.1752-1688.2010.00482.x)
1134 [1688.2010.00482.x](https://doi.org/10.1111/j.1752-1688.2010.00482.x)
- 1135 Holland, A. F., Shaughnessy, A. T., & Hiegel, M. H. (1987). *Long-Term Variation in Mesohaline*
1136 *Chesapeake Macrobenthos: Spatial and Temporal Patterns Bay* (Vol. 10, Issue 3).
- 1137 Hopkins, S. H., Anderson, J. W., & Horvath, K. (1973). *The brackish water clam Rangia cuneata*
1138 *as an indicator of ecological effects of salinity changes in coastal waters*.
- 1139 Hopkinson, C. S., & Smith, E. M. (2004). Estuarine respiration: an overview of benthic, pelagic,
1140 and whole system respiration. *Respiration in Aquatic Ecosystems*, 122–146.
- 1141 Humphreys, M. P., Lewis, E. R., Sharp, J. D., & Pierrot, D. (2022). PyCO2SYS v1.8: Marine
1142 carbonate system calculations in Python. *Geoscientific Model Development*, 15(1), 15–43.
1143 <https://doi.org/10.5194/gmd-15-15-2022>
- 1144 Irby, I. D., Friedrichs, M. A. M., Da, F., & Hinson, K. E. (2018). The competing impacts of
1145 climate change and nutrient reductions on dissolved oxygen in Chesapeake Bay.
1146 *Biogeosciences*, 15(9), 2649–2668. <https://doi.org/10.5194/bg-15-2649-2018>
- 1147 Jakubowska, M., & Normant-Saremba, M. (2015). The effect of CO₂-induced seawater
1148 acidification on the behaviour and metabolic rate of the Baltic clam *Macoma balthica*.
1149 *Annales Zoologici Fennici*, 52(5–6), 353–367. <https://doi.org/10.5735/086.052.0509>
- 1150 Jansson, A., Norkko, J., Dupont, S., & Norkko, A. (2015). Growth and survival in a changing
1151 environment: Combined effects of moderate hypoxia and low pH on juvenile bivalve
1152 *Macoma balthica*. *Journal of Sea Research*, 102, 41–47.
1153 <https://doi.org/10.1016/j.seares.2015.04.006>
- 1154 Jansson, A., Norkko, J., & Norkko, A. (2013). Effects of reduced pH on *Macoma balthica* larvae
1155 from a system with naturally fluctuating pH-dynamics. *PLoS One*, 8(6).
1156 <https://doi.org/10.1371/journal.pone.0068198>
- 1157 Kemp, W. M., Boynton, W. R., Adolf, J. E., Boesch, D. F., Boicourt, W. C., Brush, G., Cornwell,
1158 J. C., Fisher, T. R., Glibert, P. M., Hagy, J. D., Harding, L. W., Houde, E. D., Kimmel, D.



- 1159 G., Miller, W. D., Newell, R. I. E., Roman, M. R., Smith, E. M., & Stevenson, J. C. (2005).
1160 Eutrophication of Chesapeake Bay: historical trends and ecological interactions. *Marine*
1161 *Ecology Progress Series*, 303, 1–29. www.int-res.com
- 1162 Kemp, W. M., Smith, E. M., Marvin-DiPasquale, M., & Boynton, W. R. (1997). Organic carbon
1163 balance and net ecosystem metabolism in Chesapeake Bay. *Marine Ecology Progress*
1164 *Series*, 150, 229–248.
- 1165 Kroeker, K. J., Kordas, R. L., Crim, R., Hendriks, I. E., Ramajo, L., Singh, G. S., Duarte, C. M.,
1166 & Gattuso, J. P. (2013). Impacts of ocean acidification on marine organisms: quantifying
1167 sensitivities and interaction with warming. *Global Change Biology*, 19(6), 1884–1896.
1168 <https://doi.org/10.1111/gcb.12179>
- 1169 Little, S., Wood, P. J., & Elliott, M. (2017). Quantifying salinity-induced changes on estuarine
1170 benthic fauna: The potential implications of climate change. *Estuarine, Coastal and Shelf*
1171 *Science*, 198, 610–625. <https://doi.org/10.1016/j.ecss.2016.07.020>
- 1172 Llansó, R. J. (2002). *Methods for calculating the Chesapeake Bay benthic index of biotic*
1173 *integrity*. <http://www.baybenthos.versar.com>
- 1174 Llansó, R. J., & Scott, L. (2011). *Chesapeake Bay water quality monitoring program: Long-term*
1175 *benthic monitoring and assessment component, quality assurance project plan, 2011–2012*.
- 1176 Llansó, R. J., & Zaveta, D. (2017). *Chesapeake Bay water quality monitoring program: Long-*
1177 *term benthic monitoring and assessment component level 1 comprehensive report, July*
1178 *1984 – December 2016 (Volume 1)*.
- 1179 Marsh, A. G., & Tenore, K. R. (1990). The role of nutrition in regulating the population
1180 dynamics of opportunistic, surface deposit feeders in a mesohaline community. *Limnology*
1181 *and Oceanography*, 35(3), 710–724. <https://doi.org/10.4319/lo.1990.35.3.0710>
- 1182 Mo, C., & Neilson, B. (1994). Standardization of oyster soft tissue dry weight measurements.
1183 *Water Research*, 28(1), 243–246.
- 1184 Murphy, R. R., Kemp, W. M., & Ball, W. P. (2011). Long-term trends in Chesapeake Bay
1185 seasonal hypoxia, stratification, and nutrient loading. *Estuaries and Coasts*, 34(6), 1293–
1186 1309. <https://doi.org/10.1007/s12237-011-9413-7>
- 1187 Murphy, R. R., Perlman, E., Ball, W. P., & Curriero, F. C. (2015). Water-distance-based kriging
1188 in Chesapeake Bay. *Journal of Hydrologic Engineering*, 20(9).
1189 [https://doi.org/10.1061/\(asce\)he.1943-5584.0001135](https://doi.org/10.1061/(asce)he.1943-5584.0001135)
- 1190 Najjar, R. G., Herrmann, M., Cintrón Del Valle, S. M., Friedman, J. R., Friedrichs, M. A. M.,
1191 Harris, L. A., Shadwick, E. H., Stets, E. G., & Woodland, R. J. (2020). Alkalinity in tidal
1192 tributaries of the Chesapeake Bay. *Journal of Geophysical Research: Oceans*, 125(1).
1193 <https://doi.org/10.1029/2019JC015597>



- 1194 Nakamura, Y., & Kerciku, F. (2000). Effects of filter-feeding bivalves on the distribution of water
1195 quality and nutrient cycling in a eutrophic coastal lagoon. *Journal of Marine Systems*, 26,
1196 209–221. www.elsevier.nl/locate/jmarsys
- 1197 Newell, R. I. E. (1988). Ecological changes in Chesapeake Bay: are they the result of
1198 overharvesting the American oyster, *Crassostrea virginica*. *Understanding the Estuary:*
1199 *Advances in Chesapeake Bay Research*, 129, 536–546.
- 1200 Newell, R. I. E., & Ott, J. A. (2011). Macrobenthic communities and eutrophication. *Ecosystems*
1201 *at the Land-Sea Margin: Drainage Basin to Coastal Sea*, 55, 265–293.
1202 <https://doi.org/10.1029/ce055p0265>
- 1203 Ni, W., Li, M., Ross, A. C., & Najjar, R. G. (2019). Large projected decline in dissolved oxygen
1204 in a eutrophic estuary due to climate change. *Journal of Geophysical Research: Oceans*,
1205 124(11), 8271–8289. <https://doi.org/10.1029/2019JC015274>
- 1206 Pearson, T. H., & Rosenberg, R. (1978). Macrobenthic succession in relation to organic
1207 enrichment and pollution of the marine environment. *Oceanography and Marine Biology:*
1208 *An Annual Review*, 16, 229–311.
- 1209 Phelps. (1994). *The Asiatic Clam (Corbicula fluminea) Invasion and System-Level Ecological*
1210 *Change in the Potomac River Estuary Near* (Vol. 17, Issue 3).
- 1211 Rodil, I. F., Lohrer, A. M., Attard, K. M., Thrush, S. F., & Norkko, A. (2022). Positive
1212 contribution of macrofaunal biodiversity to secondary production and seagrass carbon
1213 metabolism. *Ecology*, 103(4). <https://doi.org/10.1002/ecy.3648>
- 1214 Rosenberg, R. (1995). Benthic marine fauna structured by hydrodynamic processes and food
1215 availability. *Netherlands Journal of Sea Research*, 34(4), 303–317.
- 1216 Rousi, H., Korpinen, S., & Bonsdorff, E. (2019). Brackish-water benthic fauna under fluctuating
1217 environmental conditions: the role of eutrophication, hypoxia, and global change. *Frontiers*
1218 *in Marine Science*, 6(JUL), 464. <https://doi.org/10.3389/fmars.2019.00464>
- 1219 Schratzberger, M., & Ingels, J. (2018). Meiofauna matters: the roles of meiofauna in benthic
1220 ecosystems. *Journal of Experimental Marine Biology and Ecology*, 502, 12–25.
1221 <https://doi.org/10.1016/j.jembe.2017.01.007>
- 1222 Schwinghamer, P., Hargrave, B., Peer, D., & Hawkins, C. M. (1986). Partitioning of production
1223 and respiration among size groups of organisms in an intertidal benthic community. *Marine*
1224 *Ecology Progress Series*, 31(2), 131–142.
- 1225 Seitz, R. D., Dauer, D. M., Llansó, R. J., & Long, W. C. (2009). Broad-scale effects of hypoxia
1226 on benthic community structure in Chesapeake Bay, USA. *Journal of Experimental Marine*
1227 *Biology and Ecology*, 381(SUPPL.). <https://doi.org/10.1016/j.jembe.2009.07.004>



- 1228 Seitz, R., Lipcius, R. N., Olmstead, N. H., Seebo, M. S., & Lambert, D. M. (2006). Influence of
1229 shallow-water habitats and shoreline development on abundance, biomass, and diversity of
1230 benthic prey and predators in Chesapeake Bay. *Marine Ecology Progress Series*, 326, 11–
1231 27.
- 1232 Shchepetkin, A. F., & McWilliams, J. C. (2005). The regional oceanic modeling system (ROMS):
1233 A split-explicit, free-surface, topography-following-coordinate oceanic model. *Ocean*
1234 *Modelling*, 9(4), 347–404. <https://doi.org/10.1016/j.ocemod.2004.08.002>
- 1235 Simon N. Wood. (2017). *Generalized Additive Models* (2nd ed.).
- 1236 Smith, M., Paperno, R., Flaherty-Walia, K., & Markwith, S. (2023). Species Distributions in a
1237 Changing Estuary: Predictions Under Future Climate Change, Sea-Level Rise, and
1238 Watershed Restoration. *Estuaries and Coasts*, 46(6). [https://doi.org/10.1007/s12237-023-](https://doi.org/10.1007/s12237-023-01219-5)
1239 01219-5
- 1240 Snelgrove, P. V. R. (1997). The importance of marine sediment biodiversity in ecosystem
1241 processes. *Ambio*, 26(8), 578–583. <https://doi.org/https://www.jstor.org/stable/4314672>
- 1242 Snelgrove, P. V. R. (1999). Snelgrove, P. V. (1999). Getting to the bottom of marine biodiversity:
1243 sedimentary habitats: ocean bottoms are the most widespread habitat on earth and support
1244 high biodiversity and key ecosystem services. *BioScience*, 42(2), 129–138. www.jstor.org
- 1245 Sousa, R., Antunes, C., & Guilhermino, L. (2008). Ecology of the invasive Asian clam *Corbicula*
1246 *fluminea* (Müller, 1774) in aquatic ecosystems: an overview. In *Annales de Limnologie-*
1247 *International Journal of Limnology* (Vol. 44, Issue 2, pp. 85–94).
1248 <https://doi.org/10.1051/limn:2008017>
- 1249 St-Laurent, P., & Friedrichs, M. A. M. (2024a). An atlas for physical and biogeochemical
1250 conditions in the Chesapeake Bay. *SEANOE*.
- 1251 St-Laurent, P., & Friedrichs, M. A. M. (2024b). On the sensitivity of coastal hypoxia to its
1252 external physical forcings. *Journal of Advances in Modeling Earth Systems*, 16(1).
1253 <https://doi.org/10.1029/2023MS003845>
- 1254 Sturdivant, S. K., Seitz, R. D., & Diaz, R. J. (2013). Effects of seasonal hypoxia on macrobenthic
1255 production and function in the Rappahannock River, Virginia, USA. *Marine Ecology*
1256 *Progress Series*, 490, 53–68. <https://doi.org/10.3354/meps10470>
- 1257 Testa, J. M., Faganeli, J., Giani, M., Brush, M. J., De Vittor, C., Boynton, W. R., Covelli, S.,
1258 Woodland, R. J., Kovač, N., & Michael Kemp, W. (2020a). Advances in our understanding
1259 of Pelagic-Benthic Coupling. In T. C. Malone, A. Malej, & J. Faganeli (Eds.), *Coastal*
1260 *Ecosystems in Transition: A Comparative Analysis of the Northern Adriatic and*
1261 *Chesapeake Bay* (pp. 147–175). Wiley. <https://doi.org/10.1002/9781119543626.ch8>



- 1262 Testa, J. M., Faganeli, J., Giani, M., Brush, M. J., De Vittor, C., Boynton, W. R., Covelli, S.,
1263 Woodland, R. J., Kovač, N., & Michael Kemp, W. (2020b). Advances in our understanding
1264 of pelagic-benthic coupling. In T. C. Malone, A. Malej, & J. Faganeli (Eds.), *Coastal*
1265 *Ecosystems in Transition: A Comparative Analysis of the Northern Adriatic and*
1266 *Chesapeake Bay* (pp. 147–175). Wiley. <https://doi.org/10.1002/9781119543626.ch8>
- 1267 Thomsen, J., Haynert, K., Wegner, K. M., & Melzner, F. (2015). Impact of seawater carbonate
1268 chemistry on the calcification of marine bivalves. *Biogeosciences*, 12(14), 4209–4220.
1269 <https://doi.org/10.5194/bg-12-4209-2015>
- 1270 Tumbiolo, M. L., & Downing, J. A. (1994). An empirical model for the prediction of secondary
1271 production in marine benthic invertebrate populations. *Marine Ecology Progress Series*,
1272 114(1), 165–174.
- 1273 Tuszer-Kunc, J., Normant-Saremba, M., & Rychter, A. (2020). The combination of low salinity
1274 and low temperature can limit the colonisation success of the non-native bivalve *Rangia*
1275 *cuneata* in brackish Baltic waters. *Journal of Experimental Marine Biology and Ecology*,
1276 524. <https://doi.org/10.1016/j.jembe.2019.151228>
- 1277 Vaquer-Sunyer, R., & Duarte, C. M. (2008). Thresholds of hypoxia for marine biodiversity.
1278 *Proceeds of the National Academy of Sciences*, 105(40), 15452–15457.
1279 www.pnas.org/cgi/content/full/
- 1280 Waldbusser, G. G., Powell, E. N., & Mann, R. (2013). Ecosystem effects of shell aggregations
1281 and cycling in coastal waters: an example of Chesapeake Bay oyster reefs. *Ecology*, 94(4),
1282 895–903. <https://doi.org/10.1890/12-1179.1>
- 1283 Weisberg, S., Ranasingiie, A., Schaffner Robert J Diaz, L. C., Dauer, D. M., & Frithsen, F. B.
1284 (1997). An estuarine benthic index of biotic integrity (B-IBI) for Chesapeake Bay.
1285 *Estuaries*, 20(1), 149–158.
- 1286 Wilson, J. G., & Fleeger, J. W. (2023). *Estuarine Ecology* (B. C. Crump, J. M. Testa, & K. H.
1287 Dunton, Eds.; 3rd ed.). Wiley.
- 1288 Wood, S. N. (2011). Fast stable restricted maximum likelihood and marginal likelihood
1289 estimation of semiparametric generalized linear models. *Journal of the Royal Statistical*
1290 *Society Series B: Statistical Methodology*, 73(1), 3–36.
1291 <https://academic.oup.com/jrsssb/article/73/1/3/7034726>
- 1292 Woodland, R. J., Buchheister, A., Latour, R. J., Lozano, C., Houde, E., Sweetman, C. J., Fabrizio,
1293 M. C., & Tuckey, T. D. (2021). Environmental drivers of forage fishes and benthic
1294 invertebrates at multiple spatial scales in a large temperate estuary. *Estuaries and Coasts*,
1295 44(4), 921–938. <https://doi.org/10.1007/s12237-020-00835-9>



- 1296 Woodland, R. J., & Testa, J. M. (2020). Response of Benthic Biodiversity to Climate-Sensitive
1297 Regional and Local Conditions in a Complex Estuarine System. In V. Lyubchich, Y. R. Gel,
1298 K. H. Kilbourne, T. J. Miller, N. K. Newlands, & A. B. Smith (Eds.), *Evaluating Climate*
1299 *Change Impacts* (Vol. 1, pp. 87–22). CRC Press.
- 1300 Zhang, Q., & Blomquist, J. D. (2018). Watershed export of fine sediment, organic carbon, and
1301 chlorophyll-a to Chesapeake Bay: Spatial and temporal patterns in 1984–2016. *Science of*
1302 *the Total Environment*, 619, 1066–1078. <https://doi.org/10.1016/j.scitotenv.2017.10.279>
- 1303 Zhang, Q., Fisher, T. R., Trentacoste, E. M., Buchanan, C., Gustafson, A. B., Karrh, R., Murphy,
1304 R. R., Keisman, J., Wu, C., Tian, R., Testa, J. M., & Tango, P. J. (2021). Nutrient limitation
1305 of phytoplankton in Chesapeake Bay: Development of an empirical approach for water-
1306 quality management. *Water Research*, 188. <https://doi.org/10.1016/j.watres.2020.116407>
- 1307 Zheng, G., & DiGiacomo, P. M. (2020). Linkages between phytoplankton and bottom oxygen in
1308 the Chesapeake Bay. *Journal of Geophysical Research: Oceans*, 125(2).
1309 <https://doi.org/10.1029/2019JC015650>
- 1310